MARTIN MARIETTA ENERGY SYSTEMS LIBRARIES
3 4456 0360654 1

CENTRAL RESEARCH LIBRARY
DOCUMENT COLLECTION

ORNL 1669
Instrumentation

THE CHARACTERISTICS OF AN ELECTRON MULTIPLIER AS A DETECTOR OF HEAVY PARTICLES

Clarence F. Barnett

CENTRAL RESEARCH LIBRARY
DOCUMENT COLLECTION

LIBRARY LOAN COPY

DO NOT TRANSFER TO ANOTHER PERSON

If you wish someone else to see this document, send in name with document and the library will arrange a loan.

OAK RIDGE NATIONAL LABORATORY
OPERATED BY
CARBIDE AND CARBON CHEMICALS COMPANY
A DIVISION OF UNION CARBIDE AND CARBON CORPORATION
UCC
POST OFFICE BOX P
OAK RIDGE, TENNESSEE

ORNL 1669

Copy No. 4

Contract No. W-7405-eng-26

THE CHARACTERISTICS OF AN ELECTRON MULTIPLIER AS A DETECTOR OF HEAVY PARTICLES

Clarence F. Barnett

DATE ISSUED

JAN 27 1954

OAK RIDGE NATIONAL LABORATORY
Operated by
CARBIDE AND CARBON CHEMICALS COMPANY
A Division of Union Carbide and Carbon Corporation
Post Office Box P
Oak Ridge, Tennessee

MARTIN MARIETTA ENERGY SYSTEMS LIBRARIES

3 4456 0360654 1

ORNL 1669
Instrumentation

INTERNAL DISTRIBUTION

1. C. E. Center
2. Biology Library
3. Health Physics Library
4-5. Central Research Library
6. Reactor Experimental Engineering Library
7-11. Laboratory Records Department
12. Laboratory Records, ORNL R.C.
13. C. E. Larson
14. L. B. Emlet (K-25)
15. J. P. Murray (Y-12)
16. A. M. Weinberg
17. E. H. Taylor
18. E. D. Shipley
19. A. H. Snell
20. F. C. VonderLage
21. R. C. Briant
22. J. A. Swartout
23. S. C. Lind
24. F. L. Culler
25. A. Hollaender
26. J. H. Frye, Jr.
27. W. M. Good
28. M. T. Kelley
29. G. H. Clewett
30. R. S. Livingston
31. K. Z. Morgan
32. T. A. Lincoln
33. A. S. Householder
34. C. P. Keim
35. C. S. Harrill
36. C. E. Winters
37. D. S. Billington
38. D. W. Cardwell
39. E. M. King
40. E. O. Wollan
41. A. J. Miller
42. J. A. Lane
43. R. B. Briggs
44. L. D. Roberts
45. R. N. Lyon
46. W. C. Koehler
47. W. K. Ergen
48. E. P. Blizard
49. M. E. Rose
50. D. D. Cowen
51. W. M. Breazeale (consultant)
52. M. J. Skinner
53. C. F. Barnett

EXTERNAL DISTRIBUTION

54. R. F. Bacher, California Institute of Technology
55-303. Given distribution as shown in TID-4500 under Instrumentation Category

DISTRIBUTION PAGE TO BE REMOVED IF REPORT IS GIVEN PUBLIC DISTRIBUTION

TABLE OF CONTENTS

CHAPTER		PAGE
I	INTRODUCTION	1
	A. Survey of Previous Work	1
	B. Statement of the Problam	6
II	PHENOMENA OF SECONDARY EMISSION	9
	A. Theoretical Explanation	9
	B. Secondary Emission from Electron Impact	14
	1. Velocity Distribution	14
	2. Incident Primary Energy	15
	3. Temperature Effect	17
	4. Surface Effect	17
	5. Absorbed Gases	19
	6. Effect of Atomic Properties	19
	7. Effect of Angle of Incidence	20
	C. Secondary Emission from Positive Ion Impact	21
III	EXPERIMENTAL APPARATUS	27
	A. Ion Source	27
	B. Vacuum System	31
	C. Beam Defining System	31
	D. Electron Multiplier	32
	E. The Electrometers	36
	F. Electrical Supplies	36

CHAPTER		PAGE
IV	PRELIMINARY MEASUREMENTS	38
	A. Magnetic Analyzer Calibration	38
	B. Calibration of Electrometers	39
V	RESULTS AND DISCUSSION	43
	A. Snell's Design	43
	B. Allen's Design	46
	1. Results Obtained for Low Energy Ions	46
	2. Results Obtained for High Energy Ions	58
	CONCLUSIONS	69
	BIBLIOGRAPHY	72

LIST OF TABLES

TABLE		PAGE
I	Maximum Secondary Emission as a Function of the Target Material and Primary Energy	16
II	Secondary Electron Emission from Nickel for Low Energy H_2^+ and D_2^+	24
III	Values of Secondary Emission as Function of Energy and Mass	25
IV	Expected Effect of Pressure on the Gain of the Multiplier	51

LIST OF FIGURES

FIGURE		PAGE
1	The Magnetic Electron Multiplier	4
2	Allen Type Electron Multiplier	5
3	The Velocity Distribution of Secondary Electrons	14
4	Secondary Electron Yield as a Function of Primary Energy for BeO	15
5	Secondary Electron Yield for Smooth and Rough Carbon	18
6	Block Diagram of Equipment	28
7	Photograph of Experimental Equipment	29
8	PIG Ion Source	30
9	Photograph of Electron Multiplier	33
10	Mass Analyzer Calibration for Low Energies	40
11	Mass Analyzer Calibration for High Energies	41
12	Circuit for Calibration of Electrometer	39
13	Multiplier Response as a Function of Grid Bias Voltage	44
14	Multiplier Response as a Function of Longitudinal Distance	45
15	Gain vs Volts per Stage	47
16	Gain vs Aging	48
17	Gain vs Pressure	50
18	Gain vs Input Current	52
19	Gain vs Particle Energy	54
20	Gain vs Mass	55

FIGURE		PAGE
21	Efficiency vs Input Current	56
22	Pulse Spectrum for Low Energy Protons	57
23	Pulse Spectrum for Alpha Particles from Po^{208}	59
24	Gain vs Energy for Various Ions for Low Activation	60
25	Gain vs Energy for Various Ions for High Activation	61
26	Pulse Spectrum for 100 and 9 kev Nitrogen Ions	63
27	Efficiency vs Counting Rate	65
28	Efficiency vs Energy for Nitrogen Ions	66
29	Efficiency vs Mass	67
30	Pulse Height Curves for N_2^+ and N^+	68
31	Pulse Height Curves for Nitrogen Ions and Nitrogen Atoms ..	70

CHAPTER I

INTRODUCTION

A. Survey of Previous Work

In 1910 it was discovered that certain metals when bombarded with high energy electrons possess the property of emitting a greater number of electrons than the number initially bombarding the surface. This phenomenon has been termed "secondary emission" and is the physical basis of the current or pulse amplifier known as the electron multiplier.

The first practical electron multiplier was designed and constructed in 1935 by Zworykin, Morton and Malter.[1] Prior to 1935 intensive investigations had been made to determine the nature of secondary emission, with the view of suppression of the emission since it is detrimental in the operation of several electronic devices (e. g., secondary emission from the grid of a triode).

The general technique employed in the first designs and incorporated in designs of the present time consists of detecting positive ions and electrons by allowing them to impinge on a metal target. Usually these targets have been sensitized by heat treatment in order to increase the number of electrons emitted. Through suitable choices of electrostatic and magnetic fields these secondary electrons are accelerated to

---

[1] U. K. Zworykin, G. A. Morton, and L. Malter, Proceedings of Institute of Radio Engineers 24, 351 (1936).

another target or dynode where each of these electrons gives rise to additional electrons. This process repeated several times results in a cascade which can be represented by the well-known formula:

$$I = I_o X^n$$

where I is current collected,

I_o is primary current,

X is the average number of emitted electrons per incident electron,

n is the number of stages of amplification (the number of dynodes).

Thus, it is clear that a high amplification factor (i. e., I/I_o) may be achieved provided X is large or the number of dynodes is great.

As mentioned above, the electron multiplier may be used to measure either current or single particles. Detectors commonly used for single particle detection are Geiger-Mueller tubes, proportional counters, or ionization chambers, all of which depend upon gaseous ionization. In recent years, special adaptations of the electron multiplier by Kallmann,[2] Coltman and Marshel,[3] and Jordan and Bell[4] are rapidly replacing these

---

[2]H. Kallmann, Scintillation Counter Symposium, Oak Ridge National Laboratory, June 1949.

[3]J. W. Coltman and F. L. Marshel, Nucleonics 1, 58 (1947).

[4]P. R. Bell and W. H. Jordan, Nucleonics 5, 30 (1949).

conventional detectors. These investigators have placed a fluorescent screen or phosphor in the path of the particle to be detected. The energy of the incoming particle is absorbed by the phosphor which fluoresces, emitting photons which strike the photo-sensitive first dynode of the electron multiplier. Using this method it is possible to count with high efficiency and also to obtain the energy spectrum of the incoming particle. This adaptation has found widespread use in the counting of alpha, beta, and gamma particles, yielding data on nuclear structure. (This type of counter is known as a "scintillation counter".) The multiplier to be described in this paper is to be distinguished from the above in that the first dynode is not photo-sensitive.

Two distinctive designs of the electron multiplier are commonly used. In the first multipliers constructed, crossed electric and magnetic fields were employed to focus and accelerate the electrons down the tube. Schematically, the general arrangement is shown in Fig. 1.

As seen in Fig. 1, the design consists of two rows of plates with the bottom row sensitized for high secondary electron emission. The top row establishes a transverse electric field, while a small potential difference is maintained between the plates of the bottom row to accelerate the electrons to sufficient energy for secondary emission. An external magnetic field, normal to the plane of the paper, is imposed at right angles to the electrostatic field established by the plates. The electrons will travel from plate to plate in cycloidal paths releasing additional

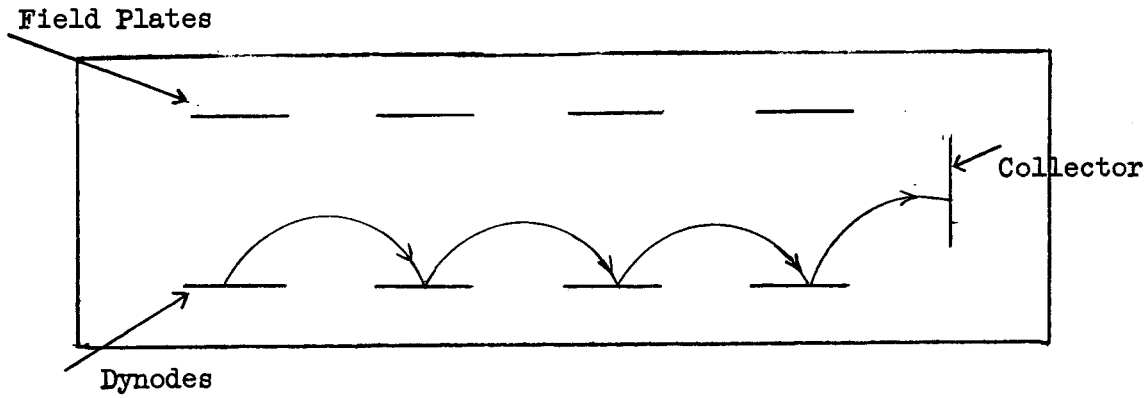

Fig. 1. Magnetic Electron Multiplier.

electrons at each impact. Lincoln Smith,[5] working at Brookhaven National Laboratory, has recently assembled a multiplier of this type with 15 stages of amplification.

The second design of the electron multiplier entails the use of only electrostatic fields to focus and accelerate electrons down the tube. Several investigators have designed and constructed multipliers of this type. However, Allen,[6,7] working at the University of Minnesota, is largely responsible for the development to its present status. To obtain large multiplication at each surface, it is necessary that the incident electron move against a field gradient near the surface of the dynode or plate. Thus, it is necessary to design a plate whose shape and potential are not

---

[5] L. Smith, "Magnetic Electron Multipliers for Detection of Positive Ions", AECU 1057 (1950).

[6] J. S. Allen, Phys. Rev. 55, 966 (1939).

[7] J. S. Allen, Rev. Sci. Instr. 18, 739 (1947).

only properly directed at the surface of the electrode but which also focuses the emitted electron to the succeeding dynode. The shape and placement of the dynodes were studied in great detail by Zworykin and Rajchman[8] and later improved by Allen. In Fig. 2 is shown a simplified diagram of the multiplier as described by Allen. The dynodes are made of beryllium-copper alloy and sensitized by heat treatment in vacuum. Eleven stages of multiplication result in an average overall multiplication of approximately 10^6 or a gain per stage of 3.8.

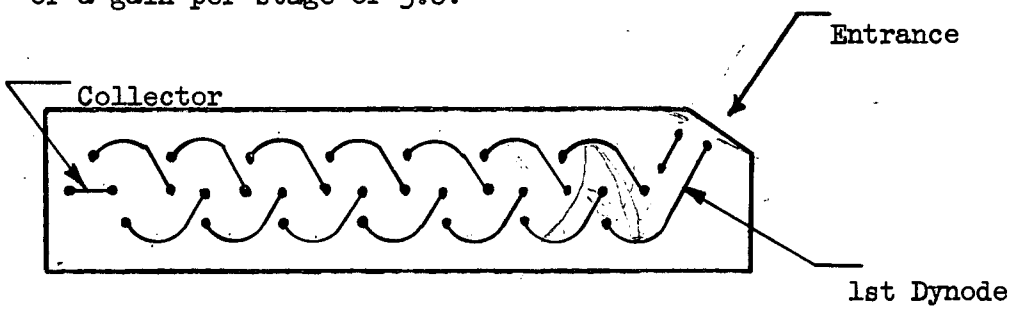

Fig. 2. Allen Type Electron Multiplier.

The advantages and disadvantages of each design are numerous. The magnetic multiplier has a smaller transit time under normal operation conditions, thus allowing higher counting rates; has no positive ion feedback, which would contribute to noise at counting rates; higher electric fields are employed resulting in larger currents before space charge effects start defocusing. It is also possible to operate the magnetic type in the presence of magnetic fields, thus enabling operation around cyclotrons and

---

[8] V. K. Zworykin and J. A. Rajchman, Proceedings of the Institute of Radio Engineers 566, September, 1939. Cf. Pierce, J. R., Bell Laboratory Record 16, 305, 1938.

other electromagnetic devices. An advantage of the pure electrostatic type is the elimination of the magnetic field, thereby eliminating the rather large and cumbersome magnet required. Also, the electrostatic multiplier is operated at lower electrical field gradients resulting in a decrease in corona discharge and surface leakage (which appear as noise).

The materials used in the construction of the multiplier (in particular the dynodes) must meet certain requirements imposed by the condition of efficient single particle detection. An important requirement of an electron multiplier is that it have a low dark current. (By "dark" current is meant all output current or pulses when there are no particles striking the first dynode.) The dark current or noise is primarily governed by the photoelectric and thermionic emission from the first dynode; therefore, the electrodes should have a high work function with a large secondary emission ratio. Since the surface is usually sensitized by heat treatment, the dynodes must also possess a high melting point. Other design requirements include rigidity to prevent microphonic vibrations of the electrodes; tightly soldered electrical contacts to reduce noise; high inter-electrode insulation to prevent surface leakage; and low collector capacitance to provide for a large voltage pulse when counting individual particles.

B. Statement of the Problem

Recently investigators, in attempting to determine the effect of radiation on the crystal structure of materials, have become aware of a serious lack of information concerning the behavior of low energy heavy particles. When radiation is absorbed by matter, the atoms or molecules

of the absorbing medium may be ejected from their normal lattice sites with considerable energy and are known as "recoil particles." These recoils lose their energy in elastic and inelastic collisions with other atoms. This process results in a local disruption of the crystal lattice which leads to changes in the properties of the material. Several laboratories have initiated research involving energy loss per collision, elastic and inelastic collision cross sections, charge exchange, and range energy relations. In view of the extremely short ranges of the recoil particles in solids, it is much more convenient to study the mechanism of energy loss of heavy charged particles in gaseous targets.

In any experiment involved in the above studies some particle detector must be used to record quantitatively the particles present under various conditions. Conventional detectors cannot be used for two reasons. One is that heavy particles of low energy possess an extremely short range thereby necessitating the use of a windowless counter. Second, the energy of the particles may be so low that ionization is very improbable, thereby eliminating all detectors depending upon gaseous ionization. The normal scintillation counter presents a possible solution; however, several factors reduce its usefulness. Since no window can be used, the scintillation crystal must be mounted in a vacuum resulting in sublimation of the crystal. This difficulty could be overcome by using a crystal such as calcium tungstate; however, ion impact upon a crystal tends to darken the region where the ion beam is striking, resulting in a gradual decrease in efficiency.

In surveying the field of instruments it was decided that a con-

ventional electron multiplier might be useful as a detector meeting the above requirements. A program was initiated to determine the effect of the various parameters upon the gain of the multiplier. If the electron multiplier is to be used as a quantitative instrument, it is necessary to know the effects of pressure, aging, input current, and multiplier voltage. Finally, since different masses at various energies are to be detected, the gain must be determined as a function of mass and energy.

Throughout this report the performance of the electron multiplier is based upon its gain or efficiency. The terminology "gain" refers to the average number of electrons collected per ion incident on the first dynode, while "efficiency" refers to the ratio of the number of output pulses measured to the number of incident ions.

CHAPTER II

PHENOMENON OF SECONDARY EMISSION

A. Theoretical Explanation

The detection of positive ions with an electron multiplier is dependent upon the phenomenon of secondary emission both from positive ion impact at the first dynode and electron impact at the succeeding dynodes. For this reason it is necessary to understand the processes involved in the liberation of the secondary electrons.

No theory capable of quantitatively predicting the yield of secondary electrons from a metal surface has yet been developed. However, it is possible to predict qualitatively the extent to which the yield may be influenced by various factors, such as primary particle energy and mass, target temperature, surface condition, time, the atomic properties and composition of the target, and the angle of incidence of the primary beam.

In deriving a theory for the yield of secondary emission, three factors are of importance in the production of the secondaries. In the first place, there must be a particle interaction between the primary electron or positive ion and the electrons of the metal. Second, in slowing down in the target the primary suffers inelastic collisions, thus one must know the probability of transferring sufficient energy to the electron to allow it to emerge from the surface of the target. Third, the depth of origin of the secondary is dependent upon the energy of the primary particle. Therefore, for the secondary to be observed,

it must move from the point of creation to the surface, still maintaining sufficient energy after collisions with the target atoms to penetrate the surface barrier. None of these three processes is completely understood, so that in any theory certain assumptions must be made in order to compare experimental results with the theory:

One of the first theories using purely classical models was proposed by Bruining.[9] A condensed form of this theory is to be found in "Advances in Electronics".[10] Briefly, it is as follows: The assumption is made that the primaries lose energy according to Whiddington's law

$$\left[eV(x)^2\right] = \left[eV(p)\right]^2 - ax$$

where $eV(x)$ is primary energy at distance x from surface,

$eV(p)$ is primary energy at surface,

a is the lattice constant.

Also, it is assumed that the rate of energy loss is proportional to the number of secondaries produced per unit path length and that the secondaries are absorbed exponentially. Then the number of secondaries emitted due to a layer of thickness dx at a depth x is

$$(1) \quad di_s = Ki_p e^{-ax} \cdot \frac{deV(x)}{dx}\, dx$$

---

[9] H. Bruining, "The Secondary Emission of Solids", Springer, Berlin.

[10] K. G. McKay, "Advances in Electronics", New York: Academic Press, p. 90 (1948).

where i_s is secondary current,

α is absorption coefficient,

i_p is primary current,

K is constant of proportionality.

Substituting the energy loss as given by the Whiddington law,

$$(2)\ di_s = \frac{a}{2} Ki_p e^{-\alpha x}(e^2V_p{}^2 - ax)^{-1/2}dx \quad .$$

If $eV(x) = 0$ in Whiddington's law, then we have the maximum depth of penetration of the particles as

$$x_{max} = \frac{e^2V_p{}^2}{a} \quad .$$

On integrating (2), we obtain

$$(3)\ i_s = 1/2\ Kai_p\int_o^{x_{max}}\left[e^2V_p{}^2 - ax\right]^{-1/2}e^{-\alpha x}dx$$

$$= Ki_p\sqrt{\frac{a}{\alpha}}e^{-r^2}\int_o^r e^{y^2}dy \ ,$$

where $r = eV\sqrt{\frac{\alpha}{a}}$ $\qquad x = \frac{e^2V_p{}^2 - (\frac{a}{\alpha})y^2}{a}$.

Taking the derivative of (3) with respect to (eV_p) and setting equal to zero, we obtain

$$\frac{di_s}{d(eV_p)} = Ki_p\left[1 - 2re^{-r^2}\int_o^r e^{y^2}dy\right] = 0.$$

Solving for $r = eV_p\sqrt{\frac{\alpha}{a}} = 0.92$ and

$$V_{pmax} = \frac{0.92}{e}\sqrt{\frac{\alpha}{a}} \quad .$$

Using known values of a and α for nickel, Bruining obtained a value $V_{pmax} = 1420$ volts as compared with the experimental value of 550 volts. This V_{pmax} is the energy of the primary particle for which the secondary emission is a maximum. A theory such as Bruining presented is inadequate in that it neglects the detailed mechanism of particle interaction and absorption.

Wooldridge[11] has applied quantum mechanics to the process of secondary emission and has derived a theory in much better agreement with experimental values than the above theory. He takes into account the binding of the valence electrons to the lattice. A beam of primary electrons of kinetic energy $\frac{\hbar k^2}{2m}$ and of momentum $\hbar/k$ travels through the lattice of the metal. According to quantum theory of solids, the lattice electron in such an energy state is excited into higher energy states as a result of the interaction with the primary electron. A certain percentage of the excited electrons will have sufficient energy to escape from the lattice. The exclusion principle is taken into account in two ways:

(1) By using Fermi statistics in summing the results over all the lattice electrons and

(2) By excluding all transitions of electrons to occupied quantum states.

The yield curves obtained directly from the theory are widely variant from the experimental curves. Closer agreement with the experimental results is achieved by a process of normalization. The disagreement

---

[11] D. E. Wooldridge, Phys. Rev. 56, 552 (1939).

between theory and experiment is probably traceable to the fact that Wooldridge considers only energy losses involved in producing secondaries, and also neglects the elastic collisions of the secondary electron. The theory predicts that a large secondary emission can be obtained for metals with a large lattice constant and a small Fermi energy. One is unable to predict from this theory whether contributions from filled bands are appreciable.

Another theory advanced by Kadyshevich[12] states that the secondaries arise from collisions with effectively free electrons of the metal. The primary particle collides with a free electron imparting to it a component of momentum in a direction normal to the direction of the particle. These electrons undergo elastic collisions with electrons and lattice ions, and some are eventually liberated from the surface. This theory fails at high energies since no account is taken of the interaction of the primaries with the lattice ions.

The hypothesis that bound electrons may be important sources of secondaries has not been investigated thoroughly. Certain qualitative arguments can be made to suggest that the bound electrons are important sources of secondaries. The arguments are:

(1) Bound electrons are much more numerous and thus for high primary energies may be important.

(2) Experimental evidence shows the yield curve as a function of energy to be very much the same as the ionization curve of gases; thus

---

[12] A. E. Kadyshevich, Journal of Physics, USSR 2, 115 (1952).

the secondaries may arise from a process of ionization in the metal.

B. Secondary Emission from Electron Impact: Experimental Results

1. Velocity Distribution

The yield of secondary electrons from metals is usually denoted by the symbol δ and is defined as the ratio of secondary electron current to the primary current. In Fig. 3 is shown a curve determined by Rudberg.[13]

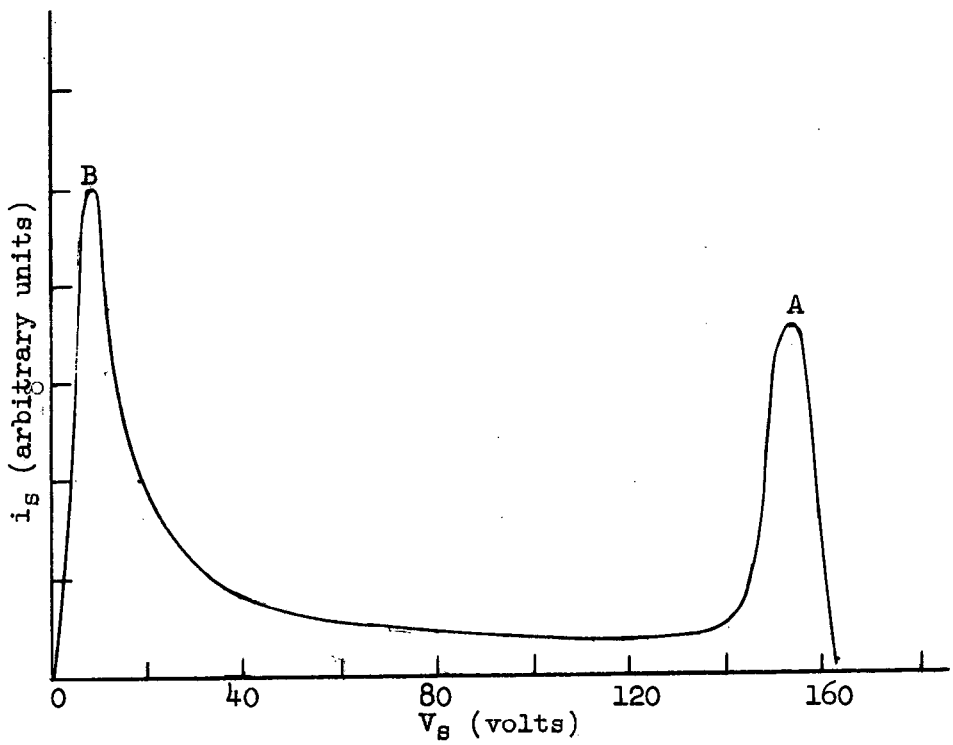

Fig. 3. Velocity Distribution of Secondary Electrons.

The curve may be interpreted as follows: The peak at point A is due to primary electrons which are elastically reflected from the target at the same energy (i. e., V_s = incident velocity). These electrons are

[13]E. Rudberg, Phys. Rev. 50, 138 (1936).

known as reflected electrons. A maximum at point B results from the true secondary electrons, with the curve being very close to a Maxwellian distribution. The part of the curve between peak A and the Maxwellian distribution is produced by inelastically reflected primaries. The total yield is usually reported (i. e., the integral of Fig. 3).

2. Incident Primary Energy

The general shape of the curve of yield versus the primary energy is practically the same for all target materials. Fig. 4[14] shows the

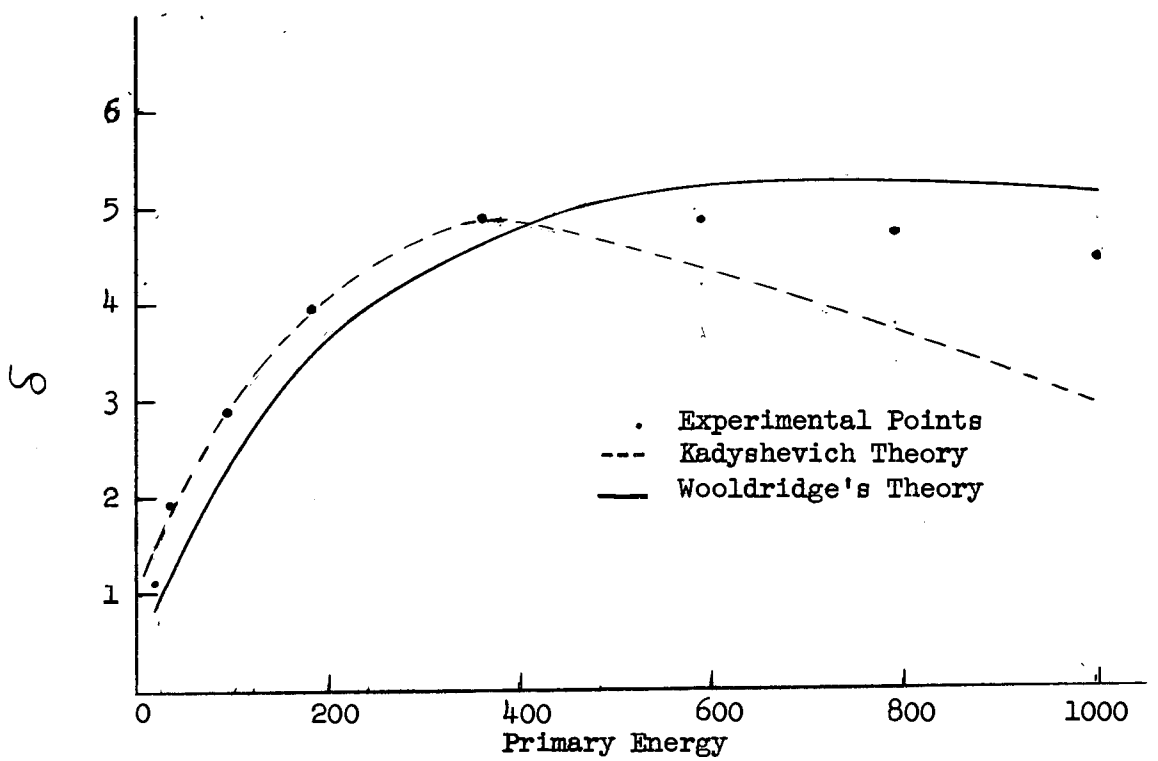

Fig. 4. Secondary Electron Yield as a Function of Primary Energy for BeO.

[14] H. S. W. Massey and E. H. S. Burhop, "Electronic and Ionic Impact Phenomena," Oxford University Press, 1952, p. 306.

variation in yield for BeO. It is seen that the yield increases to a maximum at approximately 600 volts and then gradually decreases. Also shown are the values predicted by the theories of Wooldridge and Kadyshevich. For pure metals the value of δ_{max} is usually between 1.0 and 5.5, while for compounds the values are usually greater, being as high as 11 for compound surfaces of cesium. Table I from Kollath[15] shows the value of δ_{max} and the incident energy at the maximum for a number of materials.

Table I

Maximum Secondary Emission as a Function of the Target Material and Primary Energy

Target	δ_{max}	V_{pmax}
Cesium Compound	8.5	400-600
Be	5.4	600
Al	2.4	400
Pl	1.52	1000
Au	1.45	780
W	1.33	625
Ta	1.3	625
Cu	1.27	~ 600
C	0.6-1	600
Fe	1.27	400

[15] R. Kollath, Ann. de Physik 32, 285 (1938).

3. Temperature Effect

Wooldridge[16] has studied in detail the dependence of secondary emission on temperature. Previous workers had shown that secondary emission was insensitive to temperature, however, Wooldridge has detected changes of 1 to 2 per cent for iron. The measurements indicate no change in secondary emission for iron up to 200°C. Above 200°C the coefficient decreases slowly until at 900°C an abrupt change occurs, probably due to a change in the crystalline structure of the iron. This small change was contrary to that predicted from theory in that it was expected that the number of secondaries would increase roughly as the lattice constant, a, (i. e., the same as the volume coefficient of expansion). It was concluded that if there is an increase in the production of secondaries by temperature effects, then most of the electrons are absorbed before leaving the surface.

4. Effect of the Surface

Much of the work that has been done with secondary electron emission is unreliable since only a few investigators have made any attempt to control the surface condition. This is especially true for metals which oxidize readily to form a compound with properties entirely different from the metal. Also, the mechanical condition of the surface seems to play a predominant role in the emission properties. This has been explained qualitatively by assuming a rough surface to be composed of many wells. If an electron is emitted from the bottom of one of these wells,

---

[16] D. E. Wooldridge, Phys. Rev. 58, 316 (1940).

there is a high probability that it will be absorbed. Bruining[17] has made a study of the emission properties of lamp black and smooth carbon (Fig. 5) and has concluded that the greatest decrease in yield is obtained when the carbon granules are approximately 30A° apart.

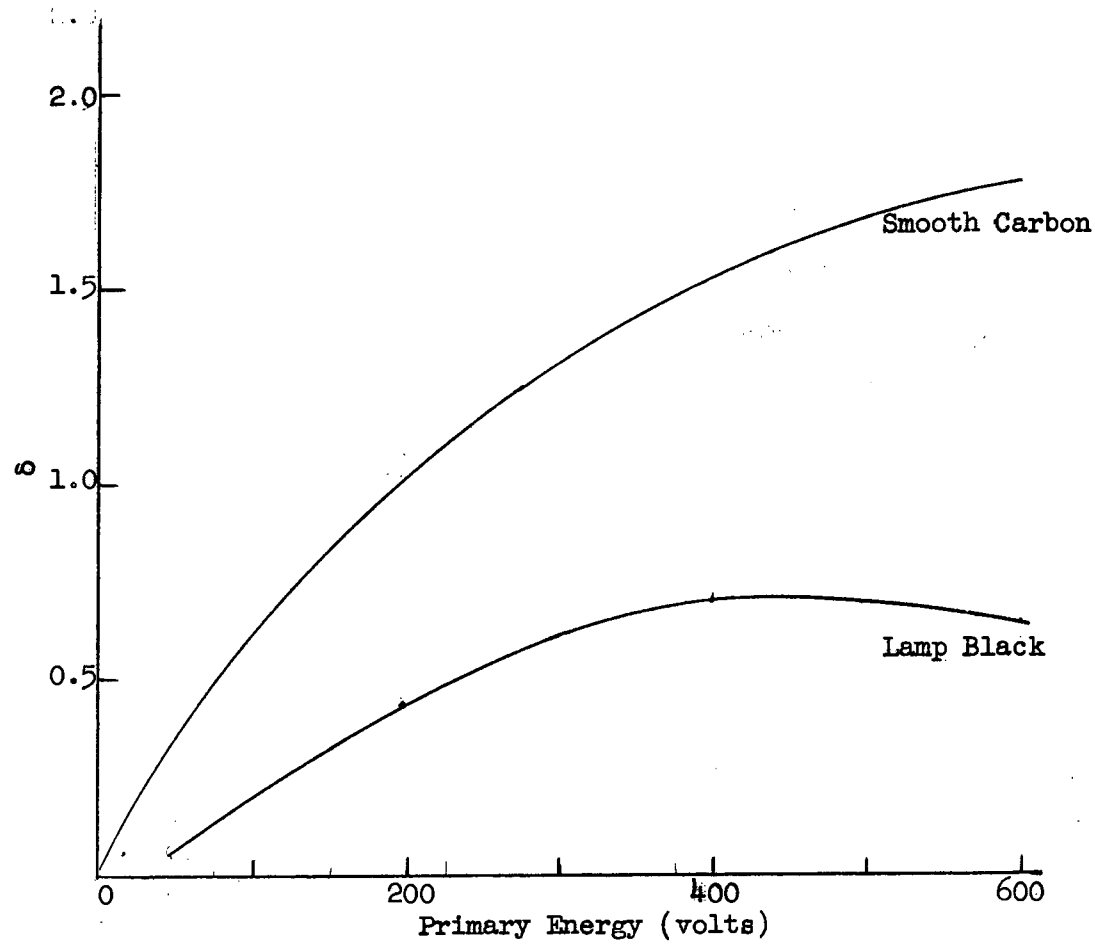

Fig. 5. Secondary Electron Yield for Smooth and Rough Carbon.

[17]H. Bruining, Philips Technical Review 3, 80 (1938).

5. Effect of Adsorbed Gases

Closely associated with surface condition is the effect of adsorbed gases on the yield. Since the amount of gases adsorbed is an unknown quantity and also since the method of removal is usually by heat treatment (which may induce crystalline changes), no quantitative statement can be made as to the effect of adsorbed gases. Generally it has been determined that the adsorbed gas increases the secondary yield appreciably. Until the emitter is completely outgassed, repeatable results cannot be obtained.

6. Effect of Atomic Properties

Certain trends have been established in the manner in which the atomic properties influence secondary emission. One would expect a change in the yield with the work function of the metal, yet from the experimental evidence available the work function plays only a minor role. A plot of yield versus the work function gives a positive slope, which is contrary to what one expects. For example, cesium with a work function of 1.81 ev has a relatively low yield of 0.7 to 0.9, while platinum with a work function of 6.27 ev has a yield of 1.8. This may suggest some other atomic property changing along with the work function.

If a plot is made of the yield versus the ionization potential of the metal, there is a direct correlation. From a classical model, if one assumes that the number of free electrons decreases as the ionization potential increases, then this suggests that secondary electrons produced within the metal may diffuse more readily to the surface if the atoms which form the lattice have a high ionization potential.

The effect of crystalline structure on yield is relatively small. Changes up to 10 per cent in yield have been detected for a change in crystal orientation. As mentioned in Section B-3, changes in yield of 1 to 2 per cent were noted as a result of change in the crystalline structure. Wooldridge and Hartman[18] have found that the change in yield between order-disorder states of the alloy Cu_3-Au is less than 1 per cent. Suhrman and Kundt[19] have studied secondary emission from thin pure metallic films in both ordered and disordered states for copper, gold and silver. The secondary emission yield increases up to 30 per cent for the ordered cases. The conclusion is usually drawn that no simple correlation has been determined between atomic properties and the yield of secondary electrons.

7. Effect of Angle of Primary Particle

Several investigators have studied the yield as a function of the primary angle and, as expected from the processes postulated in secondary emission, the yield is increased for oblique incidence, since the secondaries are formed closer to the surface, resulting in less absorption. For nearly grazing incidence the yield is often three times larger

---

[18] D. W. Wooldridge and C. D. Hartman, Phys. Rev. 58, 381 (1940).

[19] R. Suhrman and W. Kundt, Z. Phys. 120, 363 (1943).

than that for normal incidence. The Bruining law[20] for yield has been verified experimentally and is usually stated in the form

$$\sigma = ke^{(1 - \cos \theta)}$$

where θ is the angle from the normal to the surface.

C. Secondary Emission from Positive Ion Impact

The complex problem of secondary emission yield is further complicated in determining the yield from positive ion impact. For positive ion impact, not only the various parameters which were discussed for incident electrons must be considered, but also the mass and electronic configuration of the positive ions. The increased mass of the primary particle results in different type of particle interaction. Kadyshevich[21] has shown that the maximum amount of energy transferable in a collision is $4 \frac{m}{M}$ times the energy of the primary particle, where m and M are masses of electron and positive ion respectively. For low energy positive ions it would be impossible to impart sufficient energy by direct interaction with the electrons to enable them to penetrate the surface barrier.

Several processes are possible when a heavy positive ion penetrates a metal. One of the most probable is the interaction of the positive ion with the crystal lattice, giving secondary electrons. For the slow positive ions it is believed[22] that secondary emission takes place

---

[20] H. Bruining and J. H. DeBoer, Physica 6, 834 (1938).

[21] loc. cit.

[22] H. S. W. Massey and E. H. S. Burhop, loc. cit., p. 541.

in two steps: One, the positive ion captures an electron from the metal leaving the neutral particle in an excited state, and then the transition of the excited particle to the ground state emitting energy which ejects an electron from the metal. Other processes occurring from positive ion bombardment are sputtering, ions being elastically reflected, formation of metastable neutral atoms which may leave the surface, creation of negative ions by the positive ion capturing two electrons and the interaction of the positive ion with the occluded gases at the surface. All of these processes make it extremely difficult to obtain quantitative data that can be repeated by other investigators.

Due to these factors no detailed account will be presented concerning the role of the various parameters effecting the yield from positive ion impact, but rather a brief summary will be given, presenting results that several workers have obtained. Much of the early work done using artificially created ions is worthless, since it was assumed that the ions were all of the same kind, and no mass analysis was employed. Later investigations have shown that this assumption is invalid and can introduce serious errors. Using alpha particles, it was found that γ, the ratio of the number of electrons to primary positive ions, vary from 3 to 30, decreasing with increasing alpha particle energy. This decrease at high energy is probably due to the greater depth of formation, resulting in greater absorption of the electrons.

It must be remembered that the values of γ reported will vary widely since very few investigators were aware of the effect of unclean

surfaces. Usually the variation of γ with energy reaches a maximum for the lower masses while for heavy ions no maximum is obtained. For Hg[23] there is a steady increase in γ up as far as 3 Mev.

Oliphant[24] has found that for He^+ ions striking a molybdenum target the secondary emission varied with the energy of the incident ion from 0.08 to 70 in the energy range of 80 to 1000 ev. Heale and Chaffee[25] obtained practically a linear increase in emission with energy when a hot nickel target was bombarded by H_2^+ in the energy range 300 to 1000 ev. Heale,[26] in comparing the effect of H_2^+ and D_2^+, found a smaller emission from nickel for the D_2^+ than for H_2^+ ions of the same energy as shown in Table II. Heale and Houterman,[27] using an outgassed Ni target, found that for He^+ in the energy range 450 to 1650 ev the secondary emission ratio increased from 0.49 to 1.07, for Ne^+ in range 900 to 1275 ev γ increased from 0.43 to 0.57, for A^+ in range 680 to 1480, γ changed from 0.11 to 0.18. The conclusion was drawn that as the mass of the ion increases the secondary emission decreases for a given energy. Hill et al,[28] have measured the yield in the energy range 43 to 426 kev for H^+,

---

[23] L. H. Lindford, Phys. Rev. 47, 279 (1935).

[24] M. L. E. Oliphant, Proceedings of Royal Society of London A127, 373 (1940).

[25] M. Heale and E. L. Chaffee, Phys. Rev. 55, 984 (1939).

[26] M. Heale, Phys. Rev. 55, 984 (1939).

[27] M. Heale and C. Houterman, Phys. Rev. 58, 608 (1940).

[28] A. G. Hill, W. W. Buechner, J. S. Clark, and J. B. Fisk, Phys. Rev. 55, 463 (1939).

TABLE II

SECONDARY ELECTRON EMISSION FROM NICKEL
FOR LOW ENERGY H_2^+ AND D_2^+

Energy	γ	
	H_2^+	D_2^+
400	0.15	0.125
800	0.265	0.240
1200	0.375	0.305
1400	0.43	0.330

H_2^+, and He^+ bombarding targets of molybdenum, lead, aluminum and copper. Table III shows the results obtained. For protons the yield decreased, H_2^+ was nearly constant with energy, and He^+ varied slowly with energy. It is seen from the results obtained that the emission increases as the mass of particle increases. They also report a decrease in yield of approximately 50 per cent after the first two hours of operation.

Recently renewed interest in the mechanism of the loss of energy of positive ions has prompted several investigators to obtain more data to further clarify the subject.

Hagstrum[29] has made a detailed study of the electrons emitted from a clean molybdenum target by bombarding with ions of He^+, He^{++},

---

[29]H. D. Hagstrum, Phys. Rev. 89, 244 (1953).

TABLE III

VALUES OF SECONDARY EMISSION AS FUNCTION OF ENERGY AND MASS

Ion	Metal	Energy (kev)						
		78	107	142	213	284	355	426
H^+	Mo	4.1	3.77	3.27	2.76	2.35	2.18	2.01
	Cu	3.88	3.61	3.41	2.90	2.52	2.44	2.21
H_2^+	Mo	6.31	6.59	6.40	6.19	5.56	5.45	
	Cu	6.68	6.64	6.45	6.26	6.30	5.71	5.6
He^+	Mo	12.8	13.3	13.9	14.1	14.3	14.3	14.1

He_2^+ in the energy range 10 to 1000 ev. The data obtained indicates that for every He^+ ion, an electron is excited into the kinetic energy continuum with some of them being reflected at the surface barrier. Evidence is presented to show that the electron is released in an Auger type process, i. e., the excited metal ion on decaying to its ground state ionizes itself with the ejection of an electron. The metal ion is excited while the incoming ion is outside the metal surface, hence this process is commonly termed potential ejection. It was found that the number of electrons emitted is nearly independent of the kinetic energy of the primary

positive ion over the energy range studied.

Ploch[30] has made a study of lithium, neon, and potassium ions on degassed molybdenum, beryllium, and copper targets. To eliminate the effect of electronic configuration, the isotopes of the above ions were compared, and it was found that for isotopic ions of the same energy the lighter isotope always emitted more electrons than the heavier ion. From the manner in which the data are presented, the emission for ions of different elements cannot be compared. Analysis made of the data indicates a velocity dependence, since the ratio (at a given velocity) of emission for heavy isotopic ions to lighter isotopic ions is always near unity over the energy range 600 to 6000 ev. It was concluded that the only source of secondaries compatible with the data was the release of secondaries from the surface. For similar electronic configurations a simple relationship exists between the electron emission and the radius of the ion.

The inconsistencies of emission from positive ions as discussed above suggests that much more reliable experimental results must be obtained before any comprehensive theory may be established.

---

[30] W. Ploch, Zeitschrift für Physik 730, 174(1951).

CHAPTER III

EXPERIMENTAL APPARATUS

The experimental equipment used for measurements in the energy interval of 1 to 10 kev is shown in the block diagram (Fig. 6) and the photograph (Fig. 7). Briefly, it consists of an ion source to supply the ions; a beam defining system and an analyzing magnet to provide a homogeneous ion current; the electrometer to measure incident current; the vacuum system, an alpha particle source mounted on a Wilson seal; the electron multiplier; and the associated electrical equipment. For high energy measurements the beam of ions (homogeneous in mass and energy) was supplied by a conventional Cockcroft-Walton accelerator.

A. The Ion Source

The ion source[31] used in this work was developed specifically to provide an intense beam of positive ions for a Cockcroft-Walton accelerator. The essential elements of the source are shown in Fig. 8. Two circular tantalum anodes are mouted on airplane type spark plugs. This electrode assembly is flanged to a cylindrical stainless steel vacuum chamber. The vacuum seal is accomplished by means of a copper gasket. The magnetic field parallel to the axis of the electrode assembly is established by a variable electromagnet, capable of supplying field strengths up to 1000 gauss. The discharge or plasma is initiated and maintained with a standard 0 to 7.5 Kv D. C. power supply. The ions are extracted through a 1/8"

---

[31] C. F. Barnett, P. M. Stier, and G. E. Evans, Rev. Scient. Inst. 24, 394 (1953).

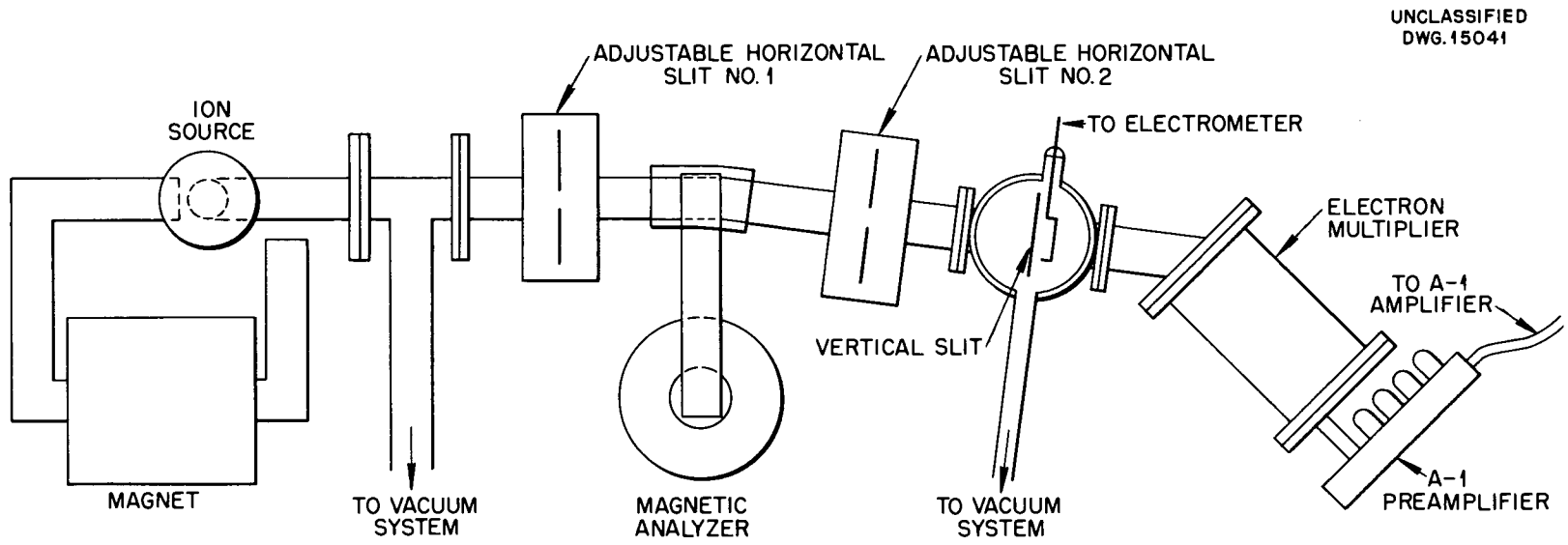

NOTE: BOTH VERTICAL SLIT AND ELECTROMETER COLLECTOR MAY BE MOVED ACROSS OR OUT OF BEAM.

Figure 6. Block Diagram of Experimental Apparatus.

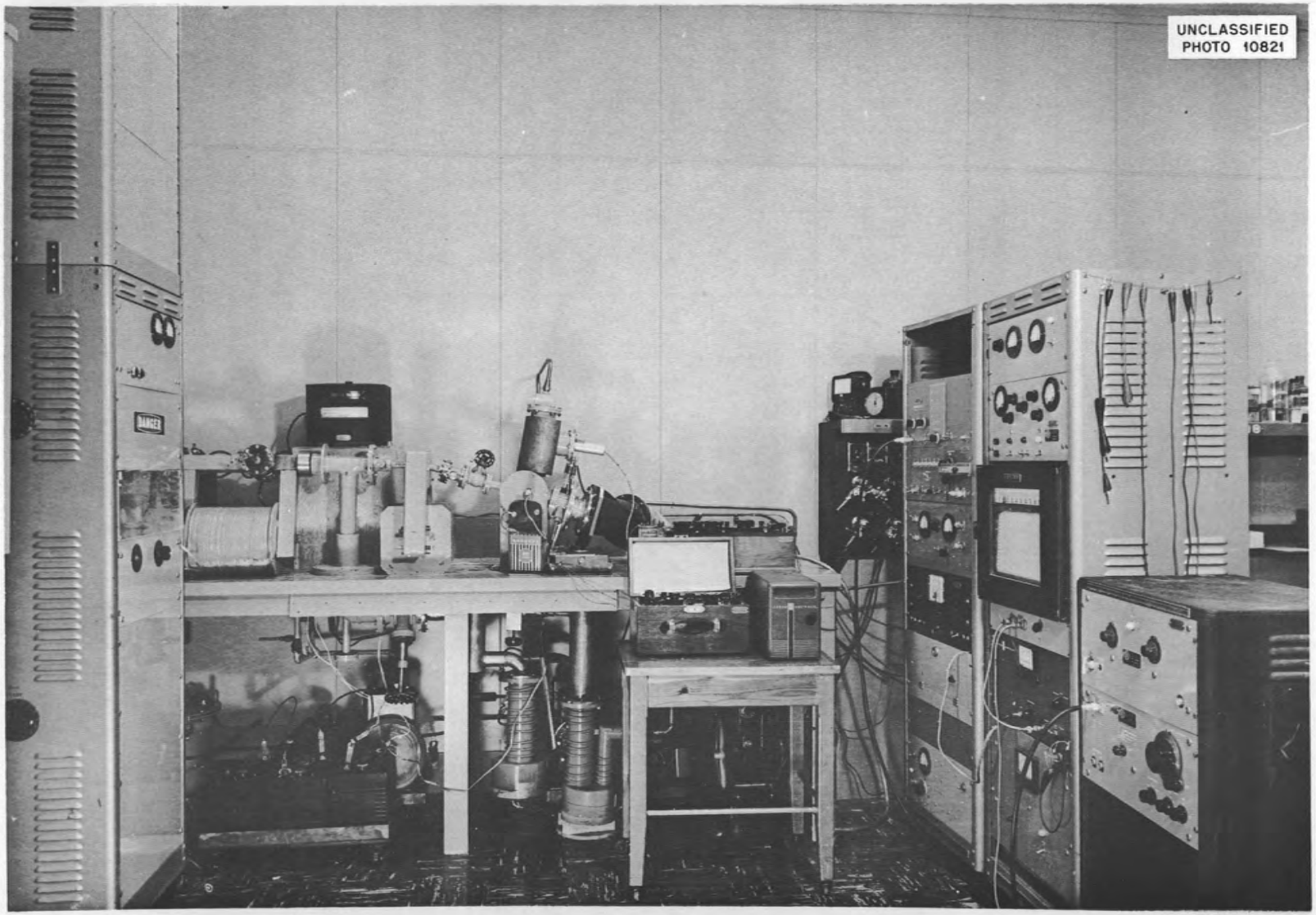

Fig. 7. Photograph of Equipment.

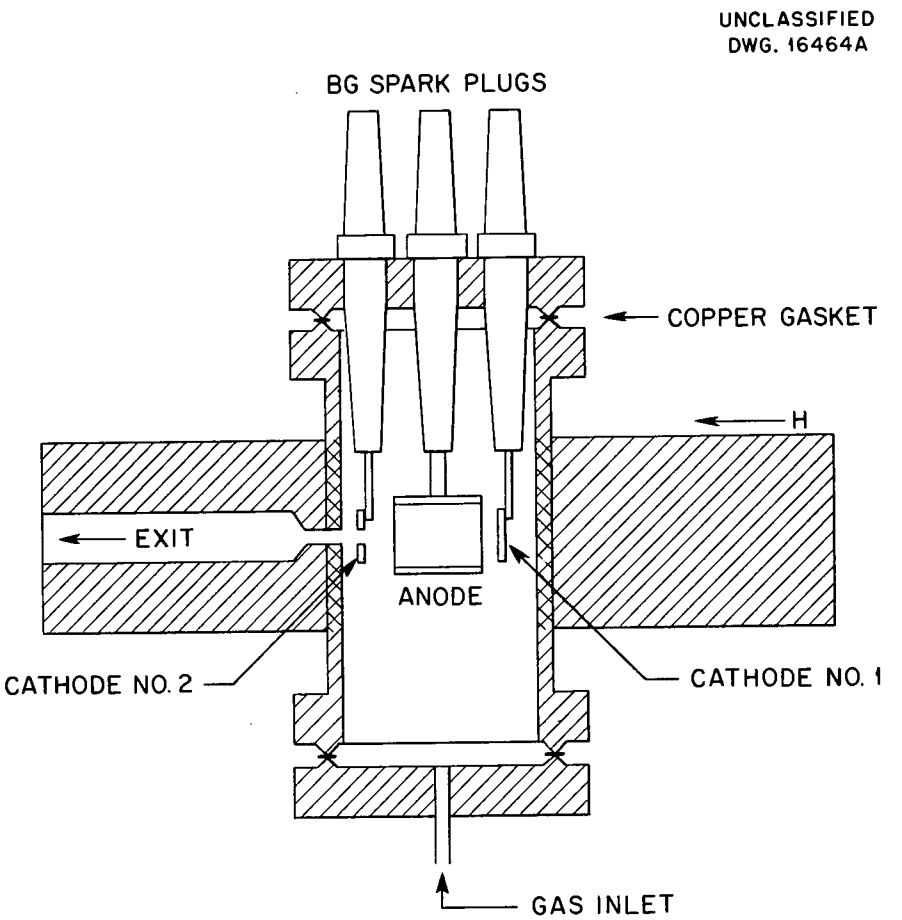

Fig. 8. PIG Ion Source.

diameter opening in one of the cathodes and are accelerated through the center of one of the pole pieces. Ion currents in excess of one milliampere have been obtained from the source. Gas consumption is approximately 2 atmospheres cc/hr. Operating life is in excess of 500 hours. Power consumption is approximately 100 watts, which could be reduced to 30 watts by replacing the electromagnet with a permanent magnet.

B. Vacuum System

The vacuum system consisted of two high vacuum oil diffusion pumps, one to maintain low pressure in the source region and the other to evacuate the multiplier region. Both pumps were VMF-260 manufactured by Distillation Products Industries. Each pump was backed by a rotary mechanical pump (Welch-Duo-Seal 1405). Between the oil diffusion pumps and the vacuum system liquid air cold traps were installed to condense oil vapor from the pumps. Octoil-S, with a vapor pressure of 10^{-8} at room temperature, was used in the diffusion pumps. All pressure measurements were made with a VG-1A ionization gauge believed to be accurate to within five per cent.

C. Beam Defining System

The beam was defined by two rotary slits, one mounted preceding the analyzing magnet with the other defining the beam after the mass analysis. Each slit consisted of a circular brass plate 1/8" thick with a horizontal slit 1/8" wide cut in the plate. By mounting these plates on rotating seals to allow axial rotation of the slit, a very highly collimated beam could be obtained. These plates also serve as the beam attenuator. To

further insure a well-collimated beam and to prevent neutral particles from entering the multiplier, a non-movable defining system was installed which consisted of two slits 1/16" wide with one mounted vertically and the other horizontally.

D. The Electron Multiplier

Two designs of the electron multiplier were constructed and tested. The first design tested is that as used by Snell,[32] while the other is basically the one designed by Allen.[33] The latter design, used in most of the experiments, is shown in photograph, Fig. 9. Essentially, Snell's design is the same as Allen's with an enlargement of the first dynode and a rearrangement of the position of the first three dynodes. Due to the increased area of the first dynode in Snell's model, it is necessary to use an entrance grid to prevent severe electric field distortion. Since the two electron multipliers are essentially of the same design, only Allen's multiplier will be discussed in detail.

All dies and templates for the multiplier were machined by the experimental machine shops at Oak Ridge National Laboratory. The dynodes were made from a commercial grade 2 per cent beryllium-copper alloy, 5 mils thick. The end pieces were fabricated of 1/4" thick teflon. The dynodes were supported between the end plates with .062" diameter nickel rods with ends threaded and terminated in rounded closed caps to hold

---

[32] A. H. Snell and L. C. Miller, "The Secondary Electron Multiplier as a Particle Counter," AECD-1956.

[33] J. S. Allen, Rev. Sci. Instr. 18, 739 (1947).

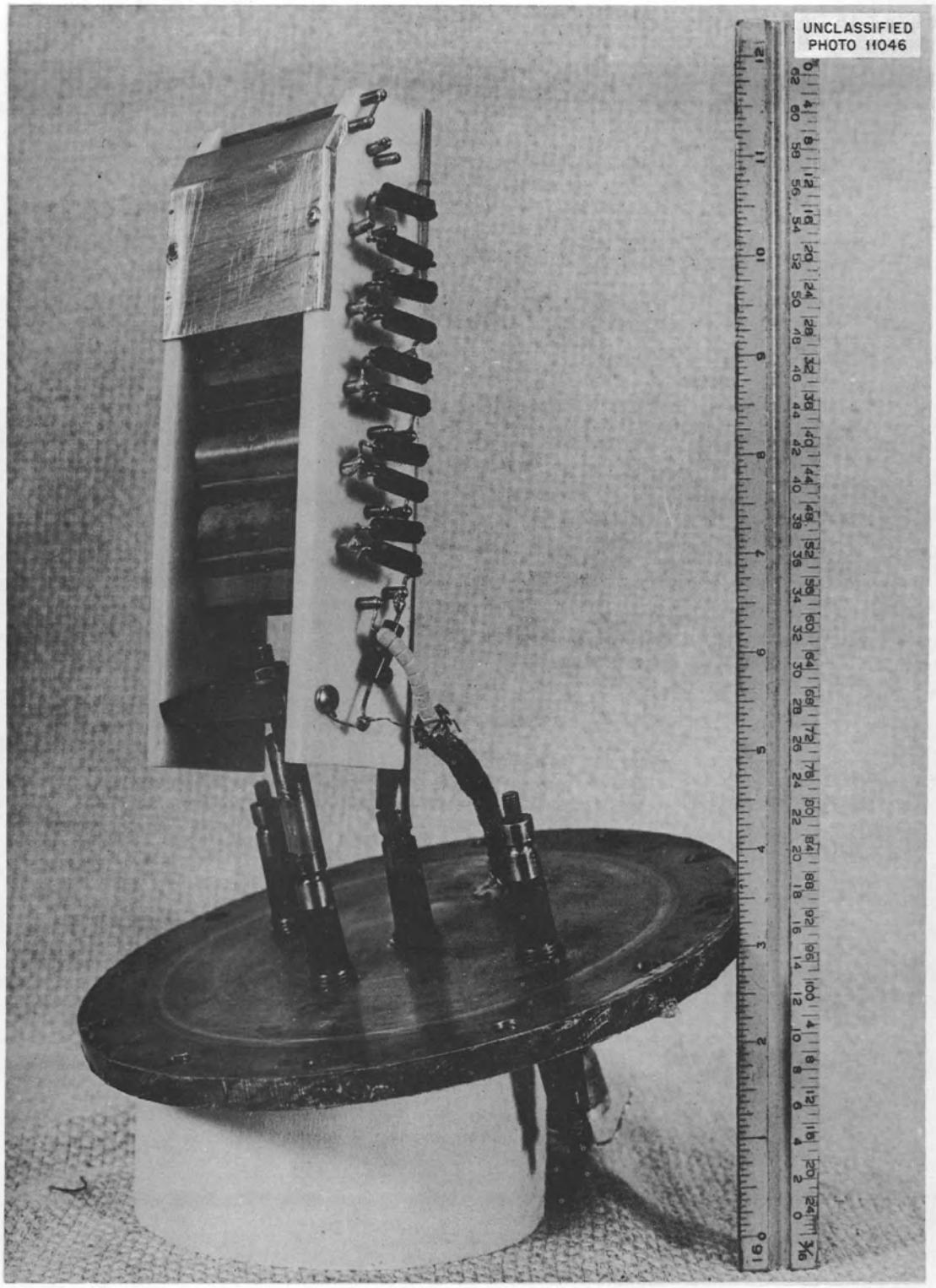

Fig. 9. Photograph of Electron Multiplier.

the assembly together while reducing corona to a minimum. External voltages were supplied through a BG-1087 airplane-type spark plug. The edges of the dynodes were rolled to allow the nickel rods to slide through. The voltage divider consisted of 1.2 megohm resistors soft-soldered to the ends of the nickel support rod. No trouble was experienced with outgassing of the resistors, but the flux used in making solid solder joints leads to some outgassing. The lead from the collector was carefully shielded and taken through the support base flange by means of a kovar seal. The capacity of the collector and output lead was 21 micro-micro farads. Aluminum plates were mounted near the front end and tied electrically to the first dynode. The purpose of these was to shield electrically the first few dynodes and to prevent positive ions from drifting in. Two multipliers were constructed with 1/2" holes drilled in the insulating end pieces to increase the pumping speed in the active region of the multiplier, since a high pressure tends to result in positive ion feedback. On later models these holes were omitted with no noticeable increase in positive ion feedback. Throughout the construction of the multiplier sharp edges and points were carefully avoided to decrease corona. The entire structure of the multiplier was mounted on a brass base flange. A soft iron vacuum housing was used to decrease effects that stray magnetic fields might have on the multiplier operation.

One great disadvantage encountered at low energies was the field distortion at the entrance of the multiplier. Since the first dynode was at potential of negative 5 kilovolts with respect to its surround-

ings, it was found necessary to attach the multiplier housing to the vacuum system with a sylphon bellows to allow adjustment of the position of the multiplier to give maximum response for various energies of incoming particles.

The method of activation of the dynodes consisted of first polishing the surface of the beryllium-copper dynodes with fine polishing paper. Then the dynodes were placed in a 4 normal solution of nitric acid until the entire surface had been etched. Following this, they were thoroughly rinsed in distilled water, then in ethyl alcohol and finally in distilled water. Immediately thereafter they were placed in a quartz tube under vacuum to outgas. Surrounding the tube was an electrical heating element whose temperature was raised to approximately 300°C to facilitate outgassing. After sufficient outgassing for the pressure to stabilize at 10^{-5} mm Hg, the temperature of the glow coil was raised until the dynodes were a dull red. After 15 minutes of this treatment the heat was removed and the dynodes were allowed to cool to room temperature. The dynodes were removed from the quartz tube, assembled onto the end plates, the voltage-dividing resistors were soldered in, and the structure placed under vacuum. No appreciable difference in sensitivity or gain was detected whether the multiplier was assembled under the atmosphere of an inert gas or under direct exposure to room conditions. Also, no noticeable change was found when the multiplier was exposed to atmospheric conditions for periods of two to three hours. The conclusion has been drawn that the sensitivity of the dynodes is not affected appreciably by exposure to air for short periods of time.

E. The Electrometers

The input current to the electron multiplier was determined by two different types of electrometers. Directly behind the vertical slit a Faraday cup was placed whose output was measured by either a balanced bridge electrometer or a vibrating reed electrometer. The balance bridge electrometer is essentially the same as that described by Lafferty and Kingdon.[34] The tube used as a GL-5674, which is a dual tube, the plate resistances of which form two legs of a balanced Wheatstone bridge. A change in the operating potential of one grid of the tube unbalances the bridge giving an indication of the potential signal on the grid. The grid resistance is of the order of 10^{11} - 10^{12} ohms, necessitating extremely high resistances in all insulations. The insulation of the Faraday cup was provided by mounting the cup on a coiled quartz rod. All leads and the electrometer tube were mounted in the same vacuum system to minimize capacitance effects. At the high grid resistance used (10^{12} ohms) the capacitance expressed in micro-micro farads equals the time constant in seconds. Thus, it is necessary to keep the capacitance to as low a value as possible. For very small currents (of the order of 10^{-16} amperes) a vibrating reed electrometer replaced the balanced bridge electrometer.

F. Electrical Equipment

For measurements at low energies (0 to 10 kev) the ions were accelerated by a conventional type D. C. power supply with the positive termi-

---

[34] J. M. Lafferty and K. H. Kingdon, Journal of Applied Physics 17, 894 (1946).

nal connected to the cathode of the ion source, the negative end being grounded. For high energies (up to 250 kev) the particles were further accelerated by a convention D. C. voltage doubler essentially the same as designed by Cockcroft and Walton.

The output current from the electron multiplier was determined by measuring the potential developed across a precision resistor inserted in the output circuit, using a high-gain D. C. microvoltmeter. At counting rates the output of the multiplier was fed to a high-gain preamplifier, the signal of which was further amplified by an Oak Ridge National Laboratory type Al linear amplifier. The counting circuit consisted of a high speed multi-scaler with an input resolving time on 1 microsecond and a scale of 4096. The output of the multi-scaler was cascaded with a scale of 64 scaler. All pulse spectra curves were obtained with a single channel differential analyzer. At high particle energies the output pulses from the multiplier were very large, making it necessary to replace the above preamplifier with a cathode follower type preamplifier of gain 0.8. The voltage to the multiplier was provided by a variable, vacuum tube regulated, 6 kilovolt supply.

CHAPTER IV

PRELIMINARY MEASUREMENTS

A. Calibration of the Magnetic Analyzer

Since the ion source is not capable of emitting a homogeneous ion beam, it was necessary to use a magnetic mass analyzer. For the low energy measurements the magnet current was supplied by three six volt storage batteries. A rotating coil gaussmeter was used to obtain the magnetic field strength. To obtain a useful curve it is convenient to plot the square of the magnetic field strength against the product of mass and the accelerating voltage. This is easily seen by equating the magnetic force to the centrifugal force:

$$Hev = \frac{mv^2}{r}$$

$$v = \sqrt{\frac{2eV}{m}}$$

$$H^2 = \frac{2e}{r^2} mV$$

where $\frac{2e}{r^2}$ is a constant of the equipment

e is electronic charge

m is particle mass

r is radius

V is accelerating voltage

H is magnetic field strength

v is particle velocity

It is seen that if the magnetic field strength and accelerating voltage are known, the mass will be fixed. In Fig. 10 the results of the mass calibration are shown for low energies, while Fig. 11 presents the curve obtained in the energy range 10 to 200 kev. The magnet used at high energies shows only slight saturation in the range used, therefore, the magnetic field is plotted as the magnet current.

B. Electrometer Calibration

The balanced bridge electrometer was calibrated using the circuit as shown in Fig. 12.

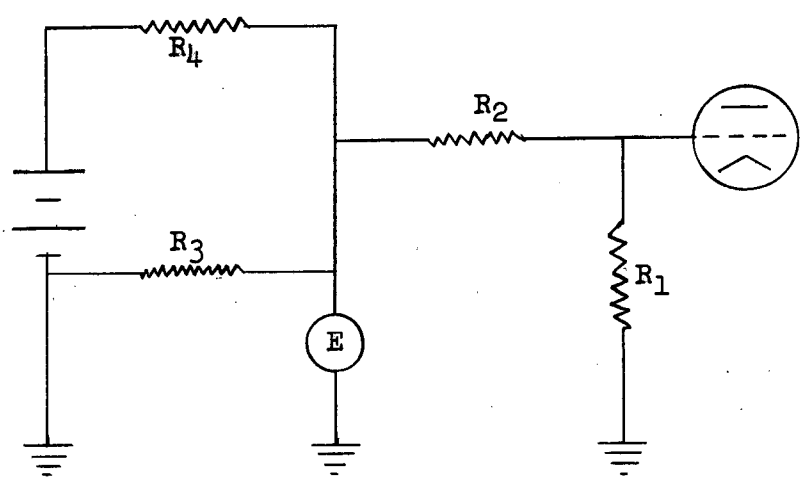

Fig. 12. Circuit for Calibration of Electrometer.

Resistance R_1, the grid resistance, is mounted inside the vacuum system with a lead coming out through a high resistance ($\sim 10^{14}$ ohms) kovar seal. The resistance R_2 was varied over the range 10^{10} to 10^{13} ohms to

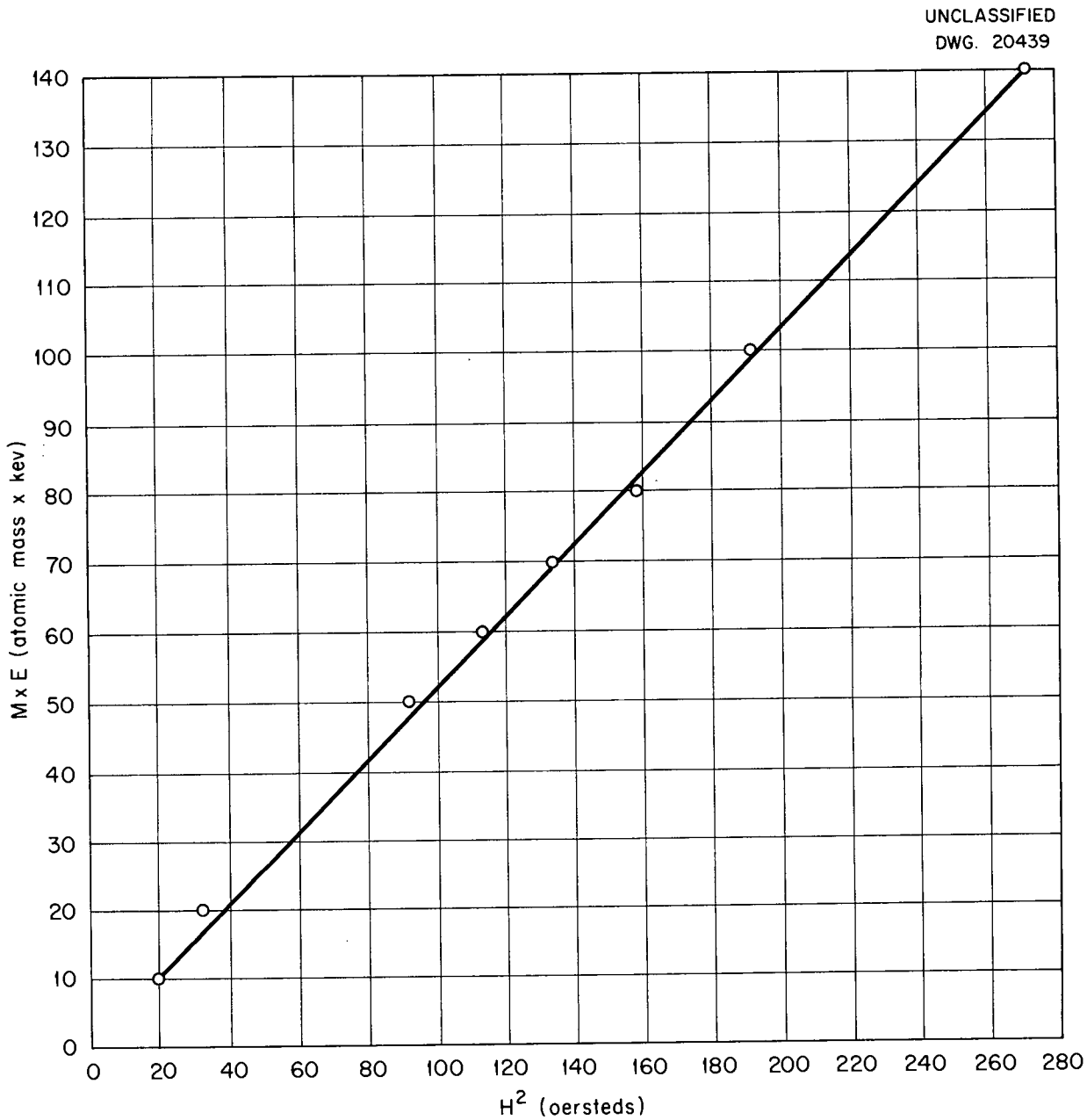

Fig. 10. Magnetic Analyser Calibration for Low Energies.

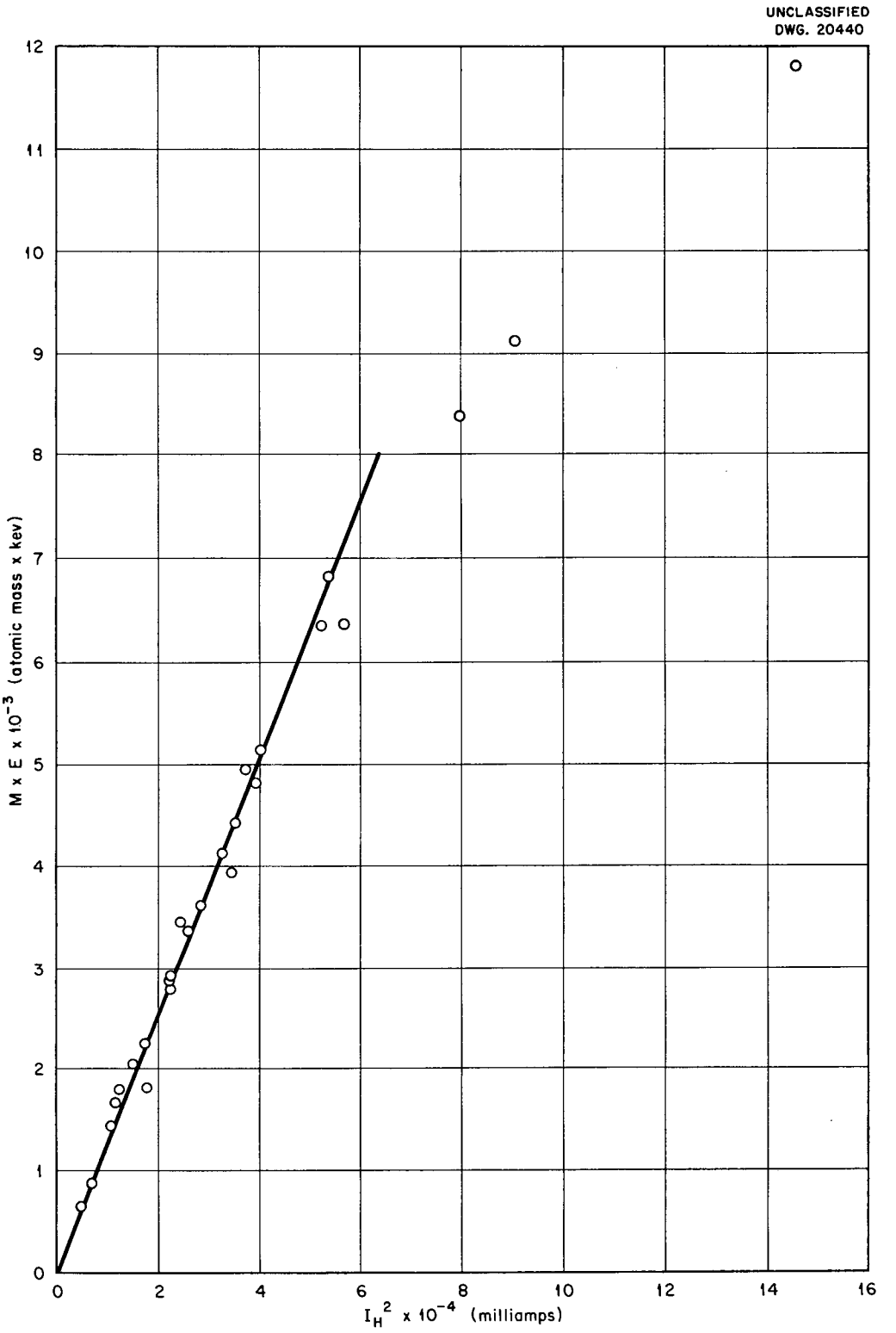

Fig. 11. Magnetic Analyzer Calibration for High Energies.

determine if any low resistances were present in the measuring circuit. No change was detected in the sensitivity of the electrometer in changing R_2, implying that the input leakage resistance was of the order of 10^{14} ohms or higher. The voltage E was measured with a high precision potentiometer capable of measuring voltages to the sixth place. R_3 and R_4 were used as voltage dividers in order to vary the impressed voltage. The Victoreen resistors (R_1 and R_2) were measured by the Instrument Division of the Oak Ridge National Laboratory. Since the resistors polarize and the resistance may change by a few per cent, it was necessary to calibrate the electrometer frequently. Using this balanced bridge electrometer currents as low as 10^{-14} amperes were easily measured with time constants of the order of 60 seconds. The range was extended by a factor of 10 by feeding the bridge output into a high gain D. C. amplifier; however, instability limited the accuracy of measurements for currents less than 10^{-15} amperes.

For lower currents a vibrating reed electrometer was used. This method involves determining the time necessary to charge a condenser a given amount. The vibrating reed electrometer was calibrated against the balanced bridge electrometer after making sure the electrometers were linear over a sufficiently wide range of currents. Currents as low as 10^{-16} amperes could be measured accurately, but considerable difficulty was encountered in obtaining reproducibility for smaller currents (e. g. 10^{-17} amps).

CHAPTER V

RESULTS AND DISCUSSION

A. Snell's Design

As described previously, Snell, et al redesigned the first two stages of the conventional electron multiplier increasing the area of the first dynode to approximately 28 sq. cm. With this large area the gain depends on the position that the beam strikes the dynode and the focusing field established by the potential gradient between the first dynode and the entrance grid. In Fig. 13 is plotted the electron multiplier response as a function of the bias voltage for H_2^+ particles of energy 8.2 kev. The two curves shown are for an overall multiplier voltage of 3.25 and 4.5 kv.

As is seen there is a shift of approximately 60 volts in the grid bias necessary for maximum response when the multiplier voltage is increased by 1.25 kv. In Fig. 14 the multiplier gain is plotted as a function of the position the ion beam strikes the dynode. The distance along the abscissa is the distance from the outer edge to the inner edge with the inner edge denoting the edge adjacent to the second dynode. Two curves are shown: (1) the bias voltage is maintained at a constant value of 200 volts as the plate is moved across the beam, (2) the bias voltage is adjusted at each position to give maximum gain. The necessary bias voltage is indicated on the graph for each position. A cursory study of this data indicates that the gain of the multiplier is influenced by the position the incident particle strikes the surface and also the bias voltage. Thus, if this type of multiplier is to be used as a quantitative detector of ions, the bias voltage must be maximized for each position the beam impinges upon the first dynode. Except for a beam of small cross section,

---

[32] Snell and Miller, loc. cit.

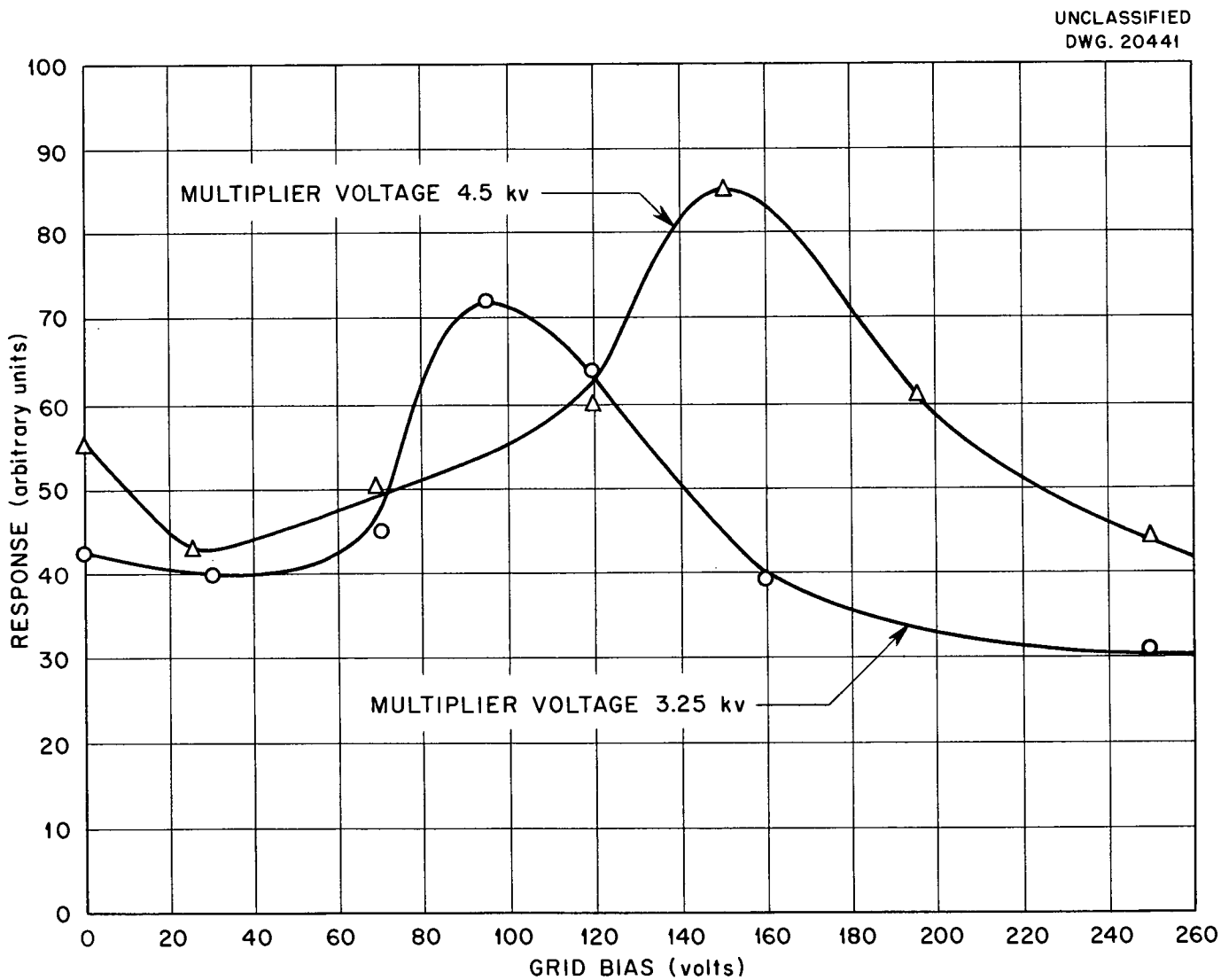

Fig. 13. Response vs. Grid Voltage.

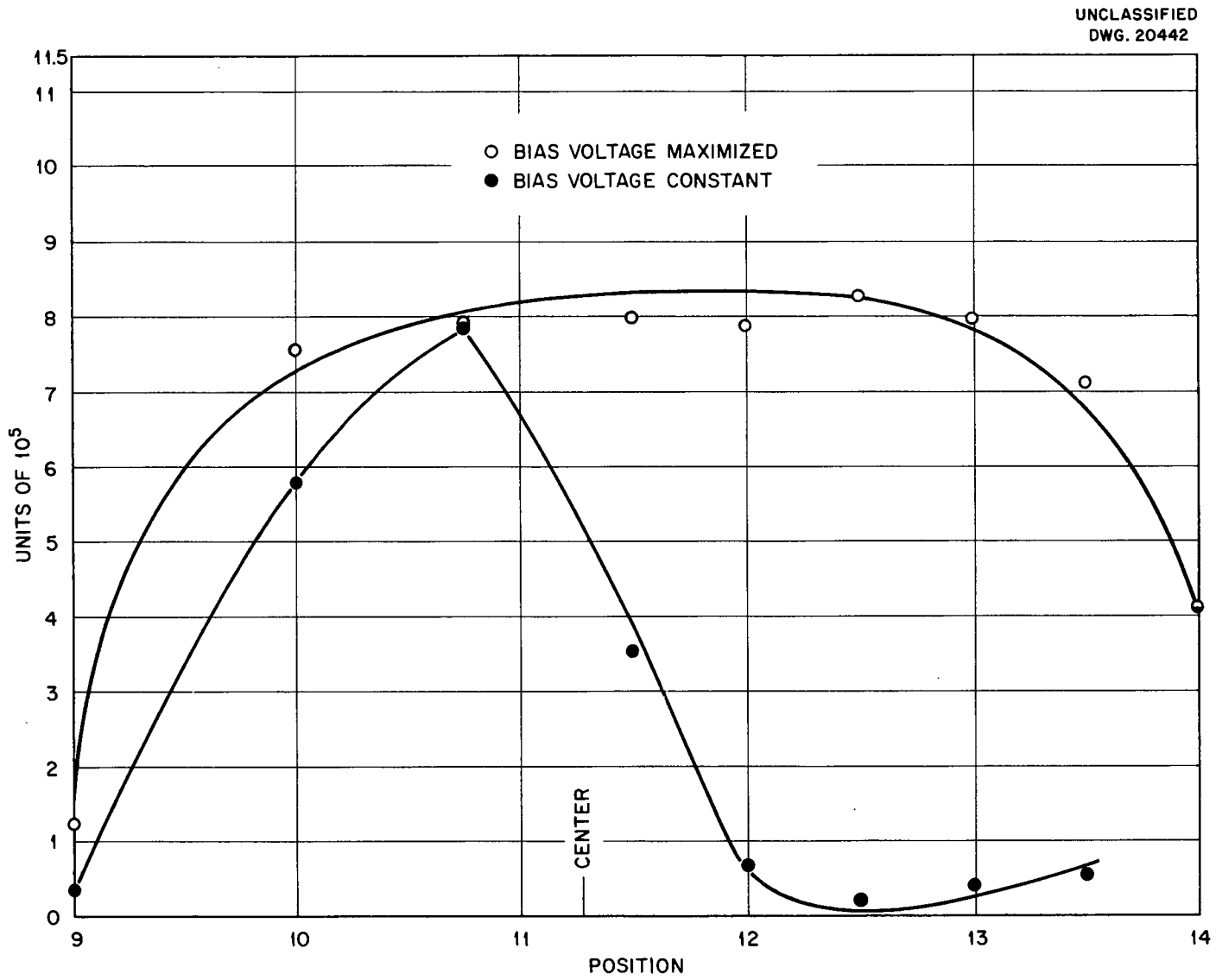

Fig. 14. Response vs. Position.

only an average gain would be determined and this would be a function of the homogeneity of the current density. Since the gain varies with position, an extremely wide distribution of output pulse heights will be obtained from the multiplier.

The difficulty encountered with this design might be overcome by shaping the entrance grid to provide a suitable electrostatic field to focus the electrons emitted from the first dynode onto the second dynode. From these considerations it was decided that the design in its present form is inadequate to enable its use as a reliable quantitative detector of positive ions.

B. Allen's Design

(1) Results Obtained at Low Energies.

The gain has been plotted as a function of multiplier voltage or volts/stage in Fig. 15. It is seen that an apparent plateau exists at approximately 500 volts/stage. With greater voltages the gain would be expected to decrease due to the greater average depth of formation of the secondary electrons. The aging effect is shown in Fig. 16. For the first few minutes of operation there is a rapid decrease in the gain followed by a slow decrease for approximately two hours; thereafter, no noticeable effect was apparent. Contrary to some previous reports, it was observed that the activation was seriously impaired by a momentary spark or glow discharge. Following a discharge the gain decreased approximately ten per cent. After a period of time the gain increased to a point where the net loss was only 2-3%. Except for such discharges or long exposure to air the gain remained constant from day to day.

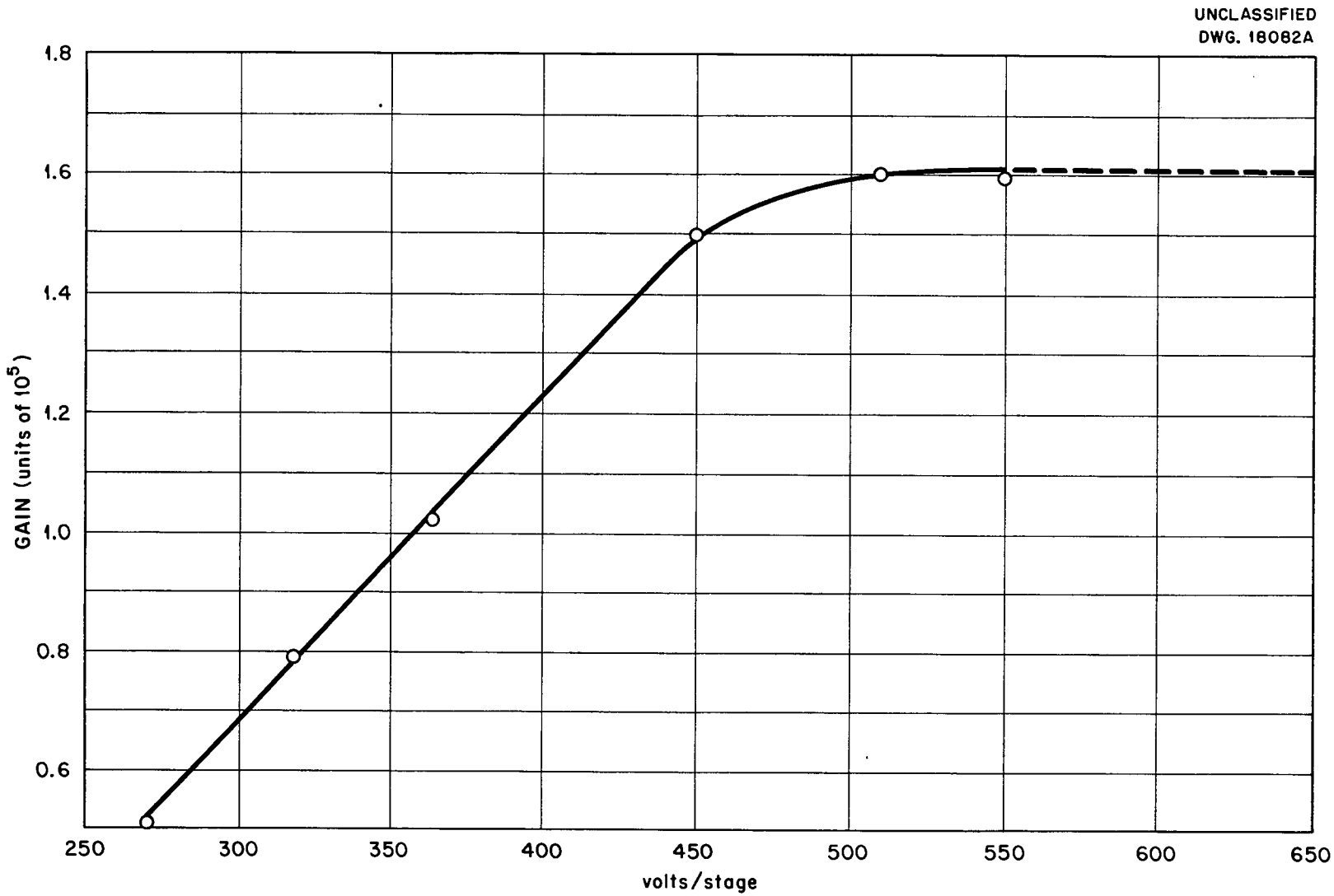

Fig. 15. Gain vs. Multiplier Voltage.

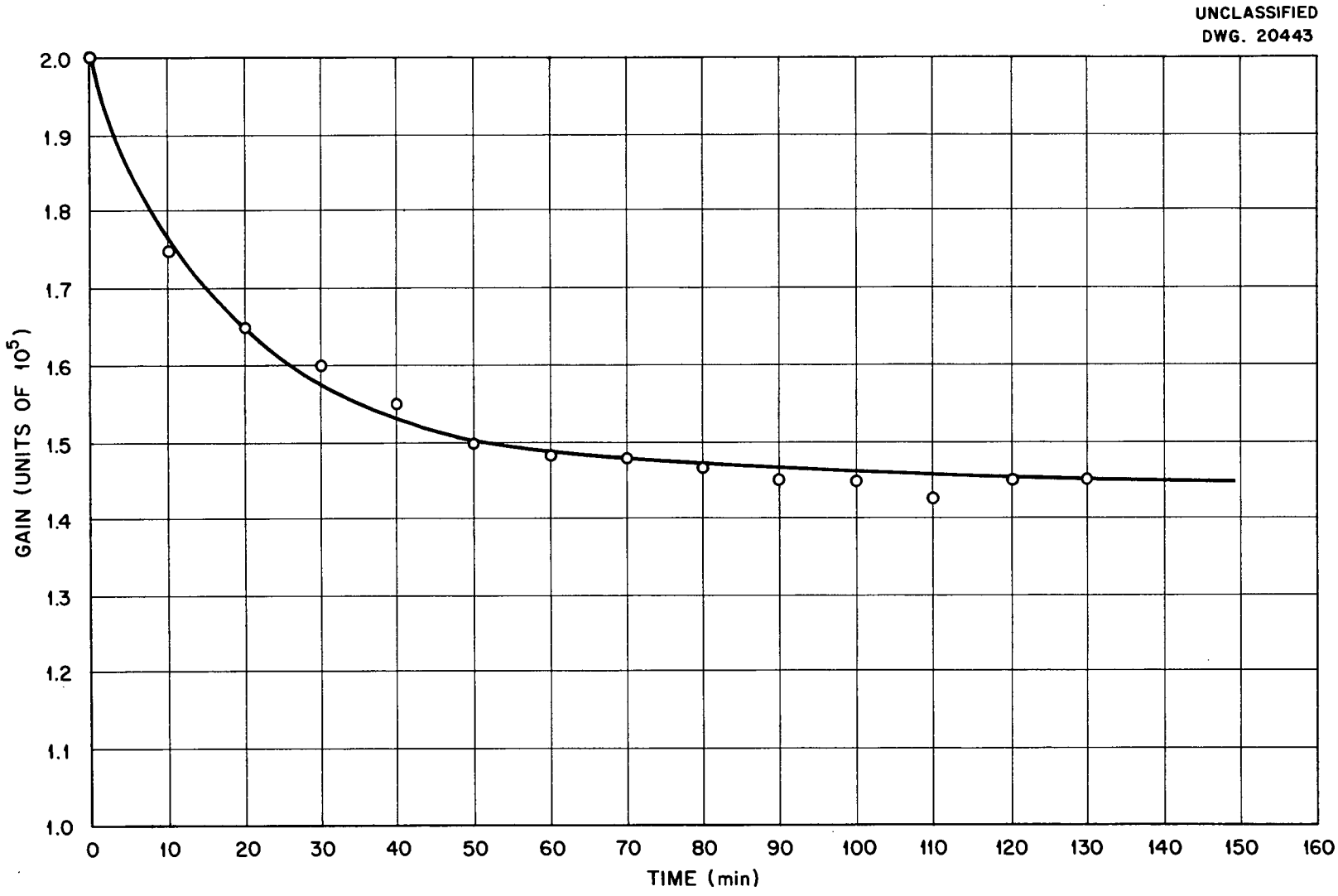

Fig. 16. Gain vs. Aging.

Fig. 17 shows the independence of the gain when the pressure in the electron multiplier region is varied between 10^{-4} and 10^{-5} mm Hg. At counting rates the pressure influences the operation in that an increase in pressure results in a rapid increase in noise or background counting rate. This probably results from corona losses around the tube. An estimate may be made of the pressure effect by a very simple calculation. The path length of an electron from one dynode to the next in the Allen type multiplier is approximately 2 cm. For a gain of 10^6 the average gain per stage is determined from

$$\gamma = X^{11}$$

$$10^6 = X^{11}$$

$$X = 3.85.$$

Using this value the total number of electrons involved in the impact of one positive ion at the first dynode is given by an expression of the form $N = 1{,}000{,}000 + 285{,}000 + 80{,}600 + \ldots\ldots\ldots$

$$= 1.4 \times 10^6,$$

or the total path length is 2.8×10^6 cm. The value given by Darrow[35] for the cross section for ionization by an electron of 100 ev average energy in air is 2.81×10^{-17} cm^2. Using this value the mean free path of the electron can be computed from the relation

$$\lambda = \frac{1}{\sigma P}.$$

---

[35] K. K. Darrow, "Electrical Phenomena In Gases" Baltimore: Williams and Williams Co., p. 142 (1932).

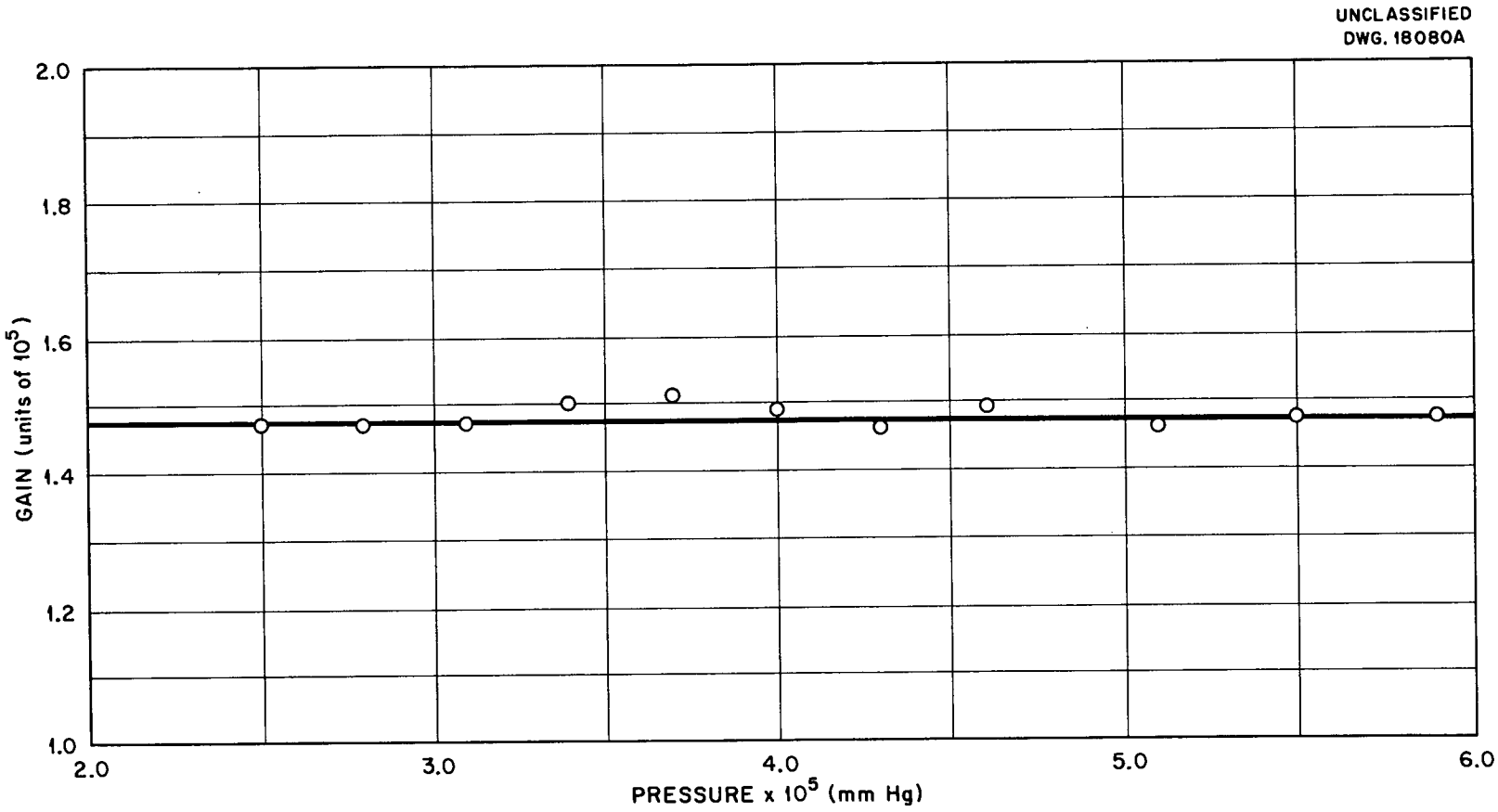

Fig. 17. Gain vs. Pressure

where λ is the mean free path

P is the pressure

σ is the cross section.

Table IV summarizes the effect of the pressure. It is assumed in the calculations that the electrons which suffer collisions are lost and that the positive ion resulting from ion pair formation liberates one electron from the preceding dynode.

TABLE IV

EXPECTED EFFECT OF PRESSURE ON THE GAIN OF THE MULTIPLIER

P (mm Hg)	λ (cm)	Number Collisions	Number Electrons Lost	Number Electrons Gained From Positive Ion	Net Loss	Per cent Loss
10^{-4}	6.8×10^{2}	4.1×10^{4}	4.1×10^{4}	3.18×10^{4}	9.2×10^{3}	0.656
10^{-5}	6.8×10^{3}	4.1×10^{3}	4.1×10^{3}	3.18×10^{3}	9.2×10^{2}	0.065
10^{-6}	6.8×10^{4}	4.1×10^{2}	4.1×10^{2}	3.18×10^{2}	9.2×10^{1}	0.007

It is thus seen that one would expect only a slight decrease in gain for operating pressures.

A determination of the possibility of current saturation is shown in Fig. 18. The gain is shown as a function of input current. There

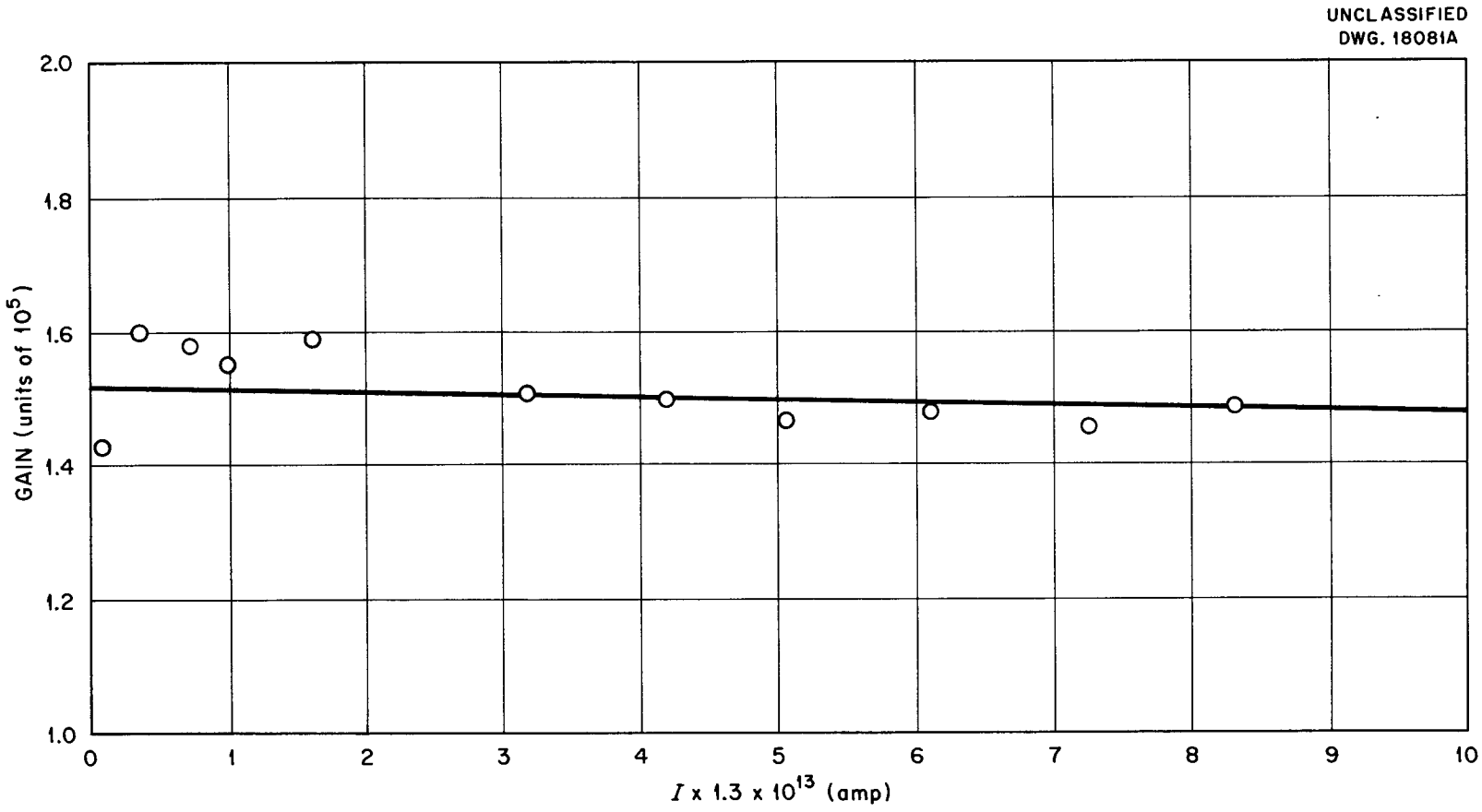

Fig. 18. Gain vs. Input Current.

apparently is little if any change in gain with the quantity of ion current up to 10^{-12} amperes. The fluctuation of the data at low currents is due to the difficulty in maintaining stable beam currents at low energies.

Fig. 19 gives the variation in gain with particle energy for protons. A difficulty in low energy ion detection was the distortion of the path due to the entrance electric field of the multiplier. For this reason it was necessary to move the multiplier with respect to the ion beam to obtain optimum gain. This probably accounts for the deviation of the data at low energies.

In Fig. 20 is plotted the gain as a function of the mass of the incident ion. It is seen that for triatomic and diatomic ions the gain is greater than that for the monatomic ions. The detailed shape of the curve has very little meaning. The gain of He^+ ions being less than that for protons contradicts the data at high energies. This observation and the unexpectedly low value for Ne^+ ions will be discussed in a later section.

The efficiency, which is the ratio of the number of output pulses to the number of incident ions, is plotted in Fig. 21 as a function of the input current. The efficiency is constant over a wide range of current. The decrease at 10^{-14} amperes arises not from the multiplier tube but rather from blocking or overloading of the linear amplifier or scaling circuit. Fig. 22 is the pulse spectrum curve taken with a single channel differential analyzer for a window or gate width of one volt. The shape of this curve indicates that a large number of the pulses are below the allowable discriminator setting of the amplifier, which is

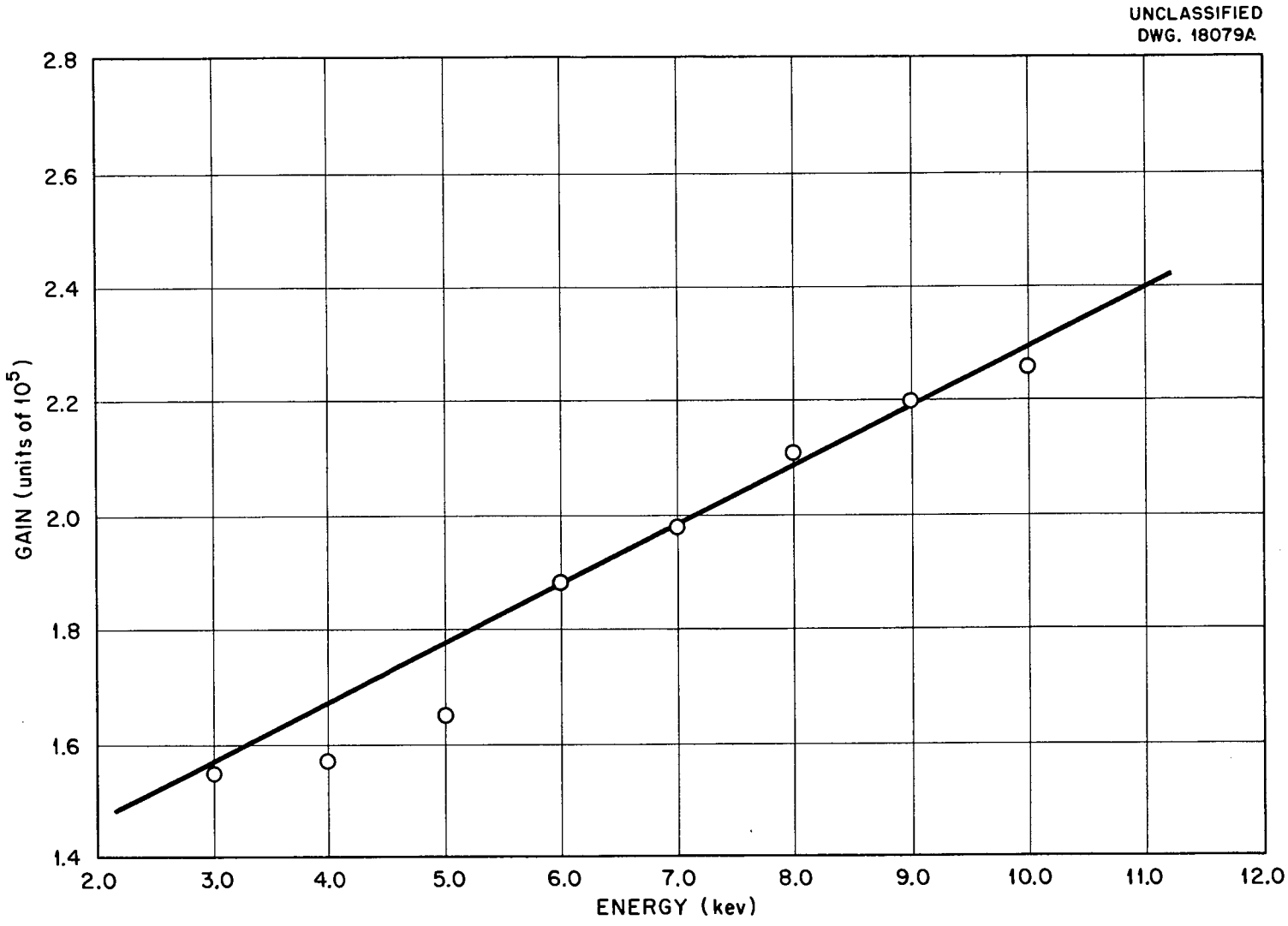

Fig. 19. Gain vs. Particle Energy.

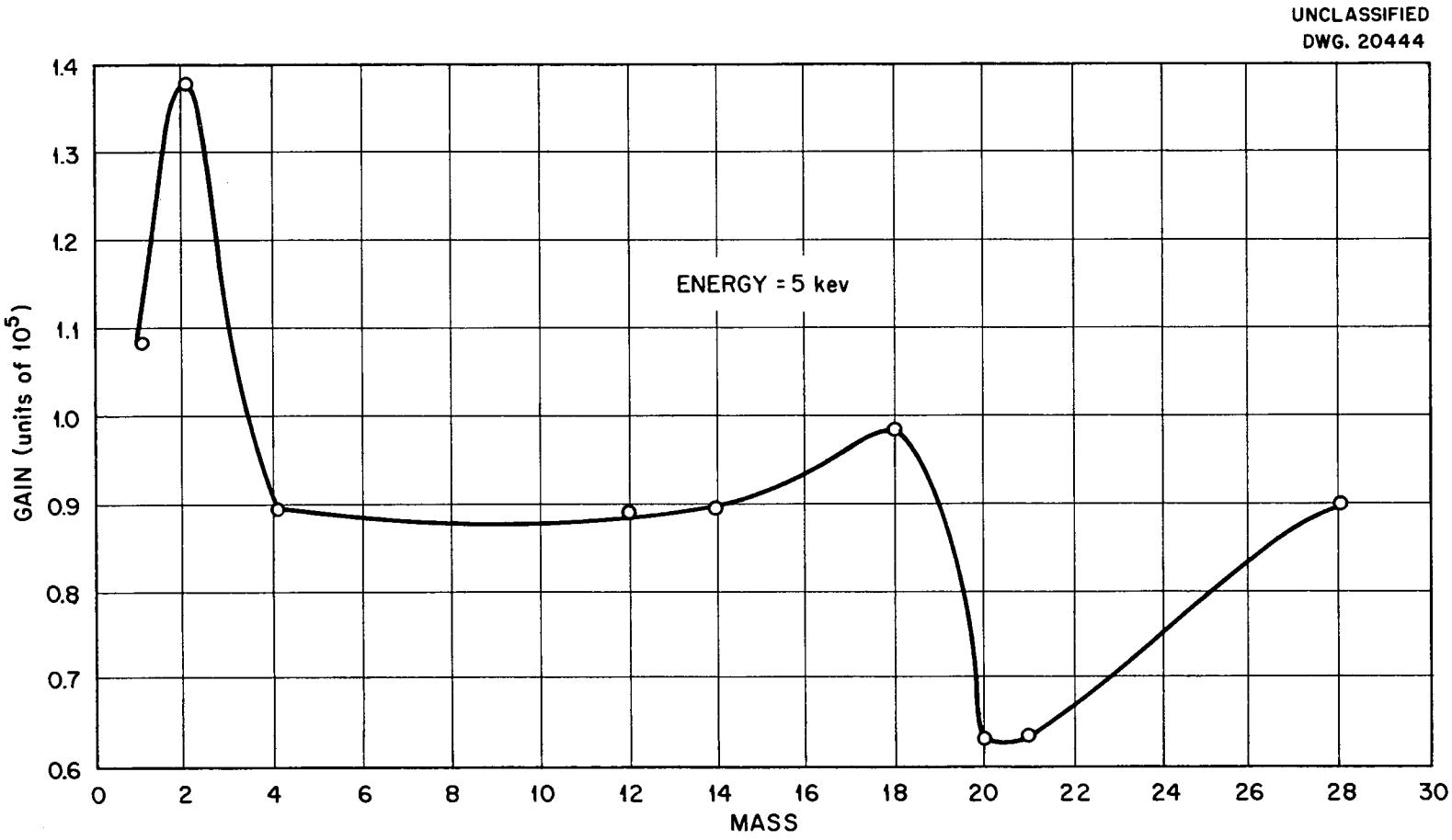

Fig. 20. Mass vs. Gain.

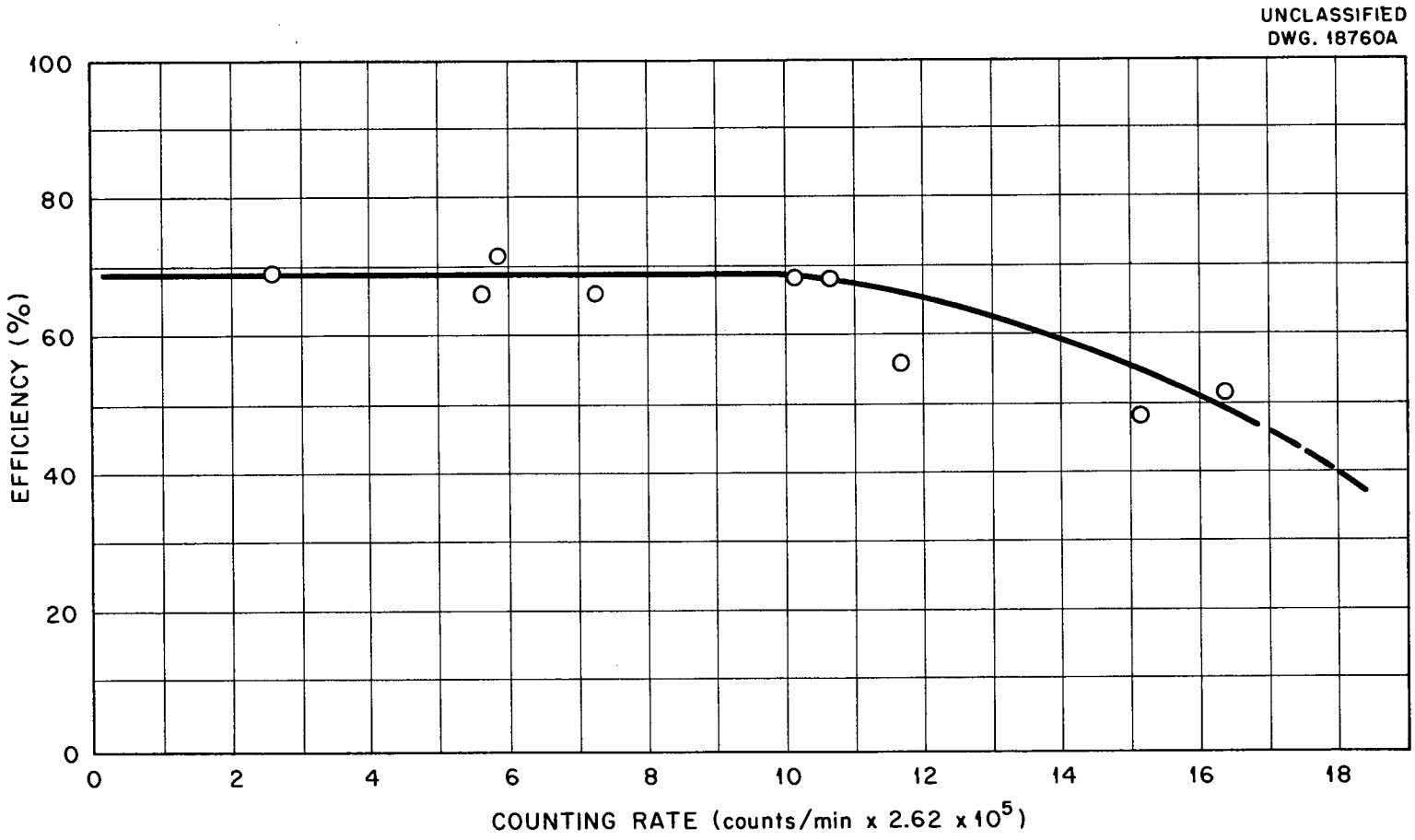

Fig. 21. Efficiency vs. Count Rate; 5-kev Protons.

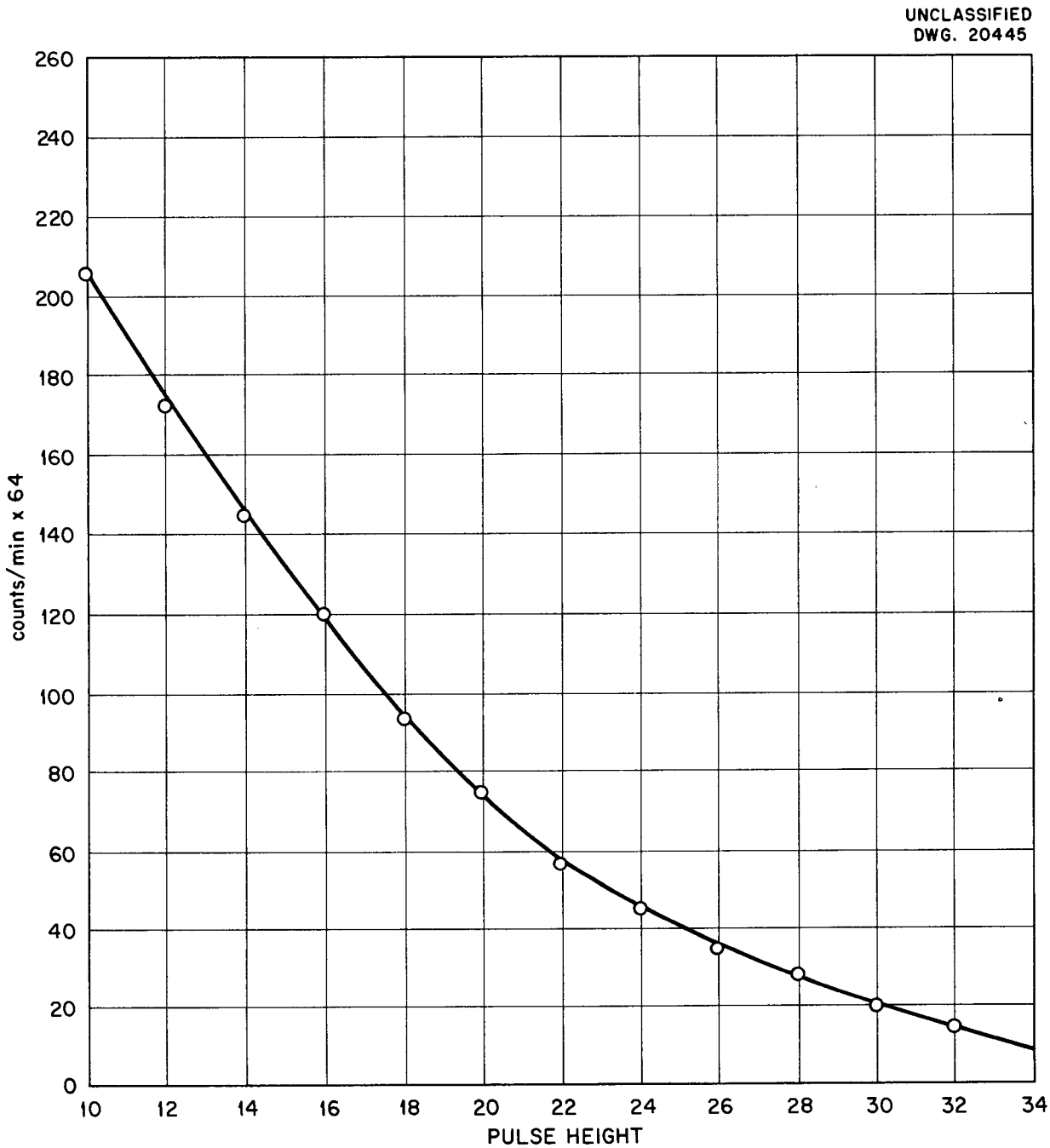

Fig. 22. Pulse Spectrum for Low Energy Protons.

determined by the noise of the circuitry. For higher efficiencies it is necessary to obtain better activation of the dynodes.

An attempt was made to count alpha particles from Po^{208}, Fig. 23. Initially the counting rate was excessive, however, investigation revealed that the negative potential of the first dynode accelerated the recoil particles from the surface of the source. To remedy this, the source was covered with a thin coating of Krylon, a plastic spray. Due to the geometry employed only a rough estimate could be made of the expected counting rate. This estimate coincided to within 20% to that as measured after coating the source.

(2) Results Obtained at High Energies.

The beam of high energy positive ions was produced by a Cockcroft-Walton accelerator capable of accelerating ions to 250 kev. Fig. 24 shows the relationship between the electron multiplier gain and the incident energy for various ion masses. These data were obtained with a gain of approximately 10^5. To determine the effect of dynode activation on the gain, the dynodes were reactivated in the usual manner and the data were taken again, as shown in Fig. 25. Here the gain is of the order of 10^6. The gain is seen to increase with the mass except for the ion Ne^+, which has a gain very nearly that of He^+. This probably results from two factors: the small radius of the Ne^+ ion, which decreases the collision cross section, and the high ionization potential of neon.

The results obtained at high energies definitely establish an increase in multiplication with increase in mass with the exception of neon. At lower energies (i. e. below 30 kev in Fig. 25) it is observed

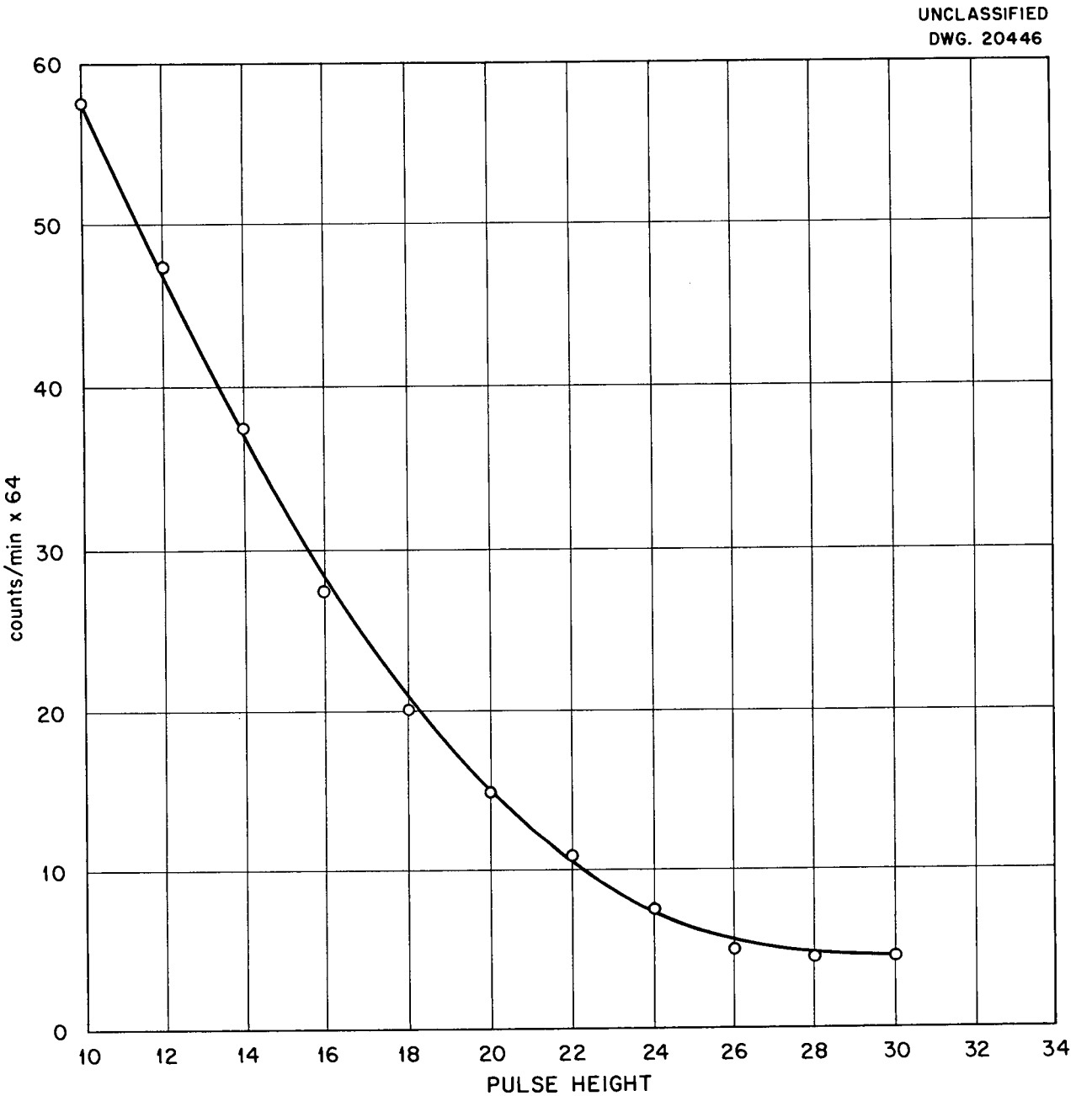

Fig. 23. Pulse Spectrum for Po^{208}.

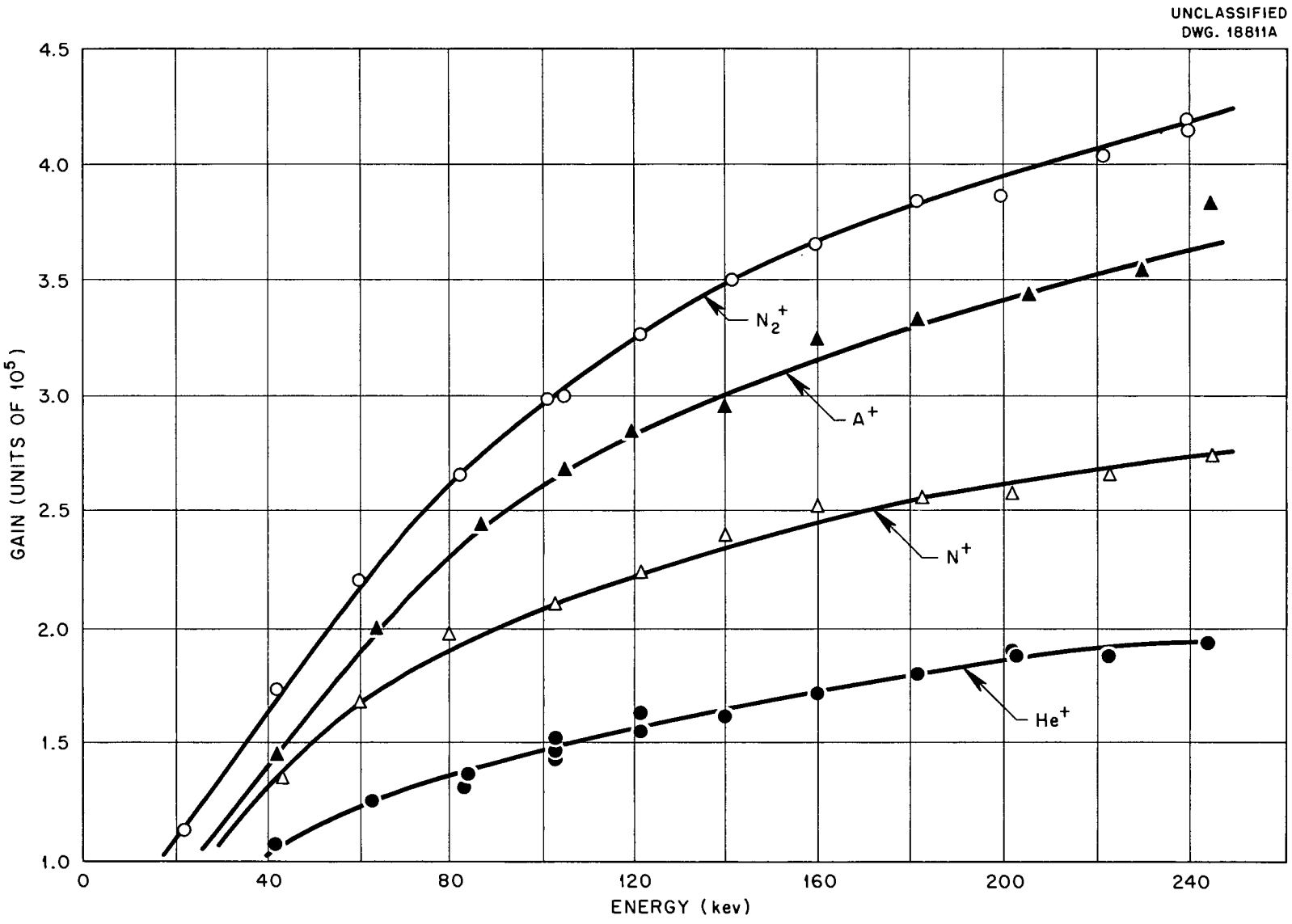

Fig. 24. Gain vs. Energy.

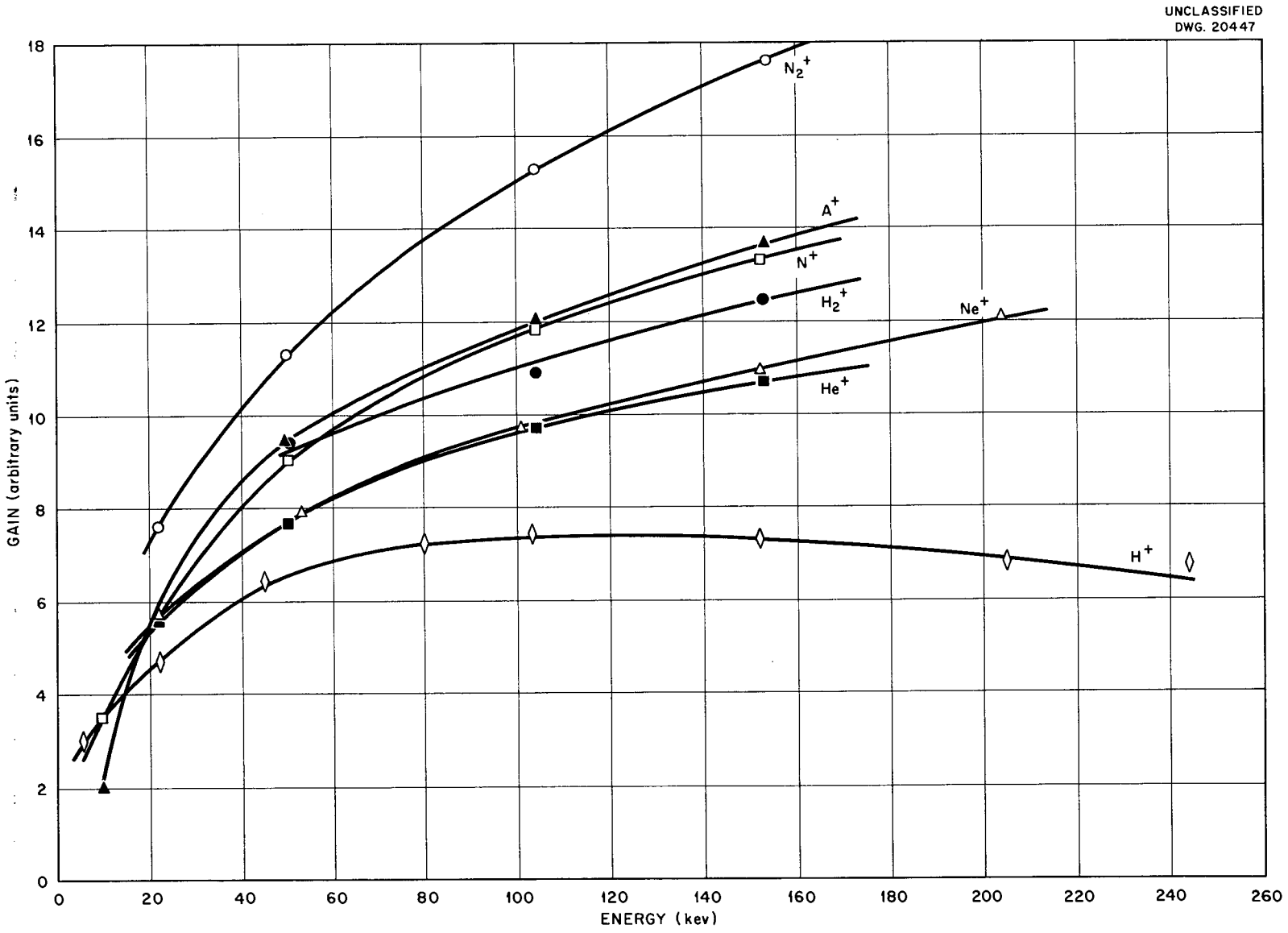

Fig. 25. Electron Multiplier Gain as a Function of Energy for Various Masses.

that the yield for light ions may become higher than the yield for heavier ions in agreement with the data as presented in section B-1. Plock[36] (also at low energy) has shown that a smaller multiplication always results from a heavier isotope than for the higher (i. e. Li^6 and Li^7). These observations suggest a strong dependence of the secondary emission on the surface condition.

The only mass showing any maximum of gain with energy is H^+. As is seen this occurs at approximately 110 kev. The general velocity dependence of secondary emission may be demonstrated by comparing this maximum with the similar maximum obtained for electrons (Fig. 15). Here the maximum number of secondary electrons per incident electron occurs at approximately 550 ev. The energy of H^+ at maximum of 110 kev divided by the relative mass of the proton is 590, thus the velocity ratio is 1.03. This is good agreement when it is realized that the detailed mechanism of energy loss is different in the two cases. These results confirm the general velocity dependence reported by Plock[37].

The pulse spectra obtained for N^+ at energies 100 kev and 9 kev are shown in Fig. 26. At the higher energy approximately 100% of the pulses are above the discriminator setting of the linear amplifier, however, with the same discriminator setting at low energy several per cent of the pulses are lost. For these measurements the gain of the amplifier is as high as is allowed by the condition that amplifier noise pulses must not be more numerous than the real pulses.

---

[36] Plock, loc. cit.

[37] Plock, loc. cit.

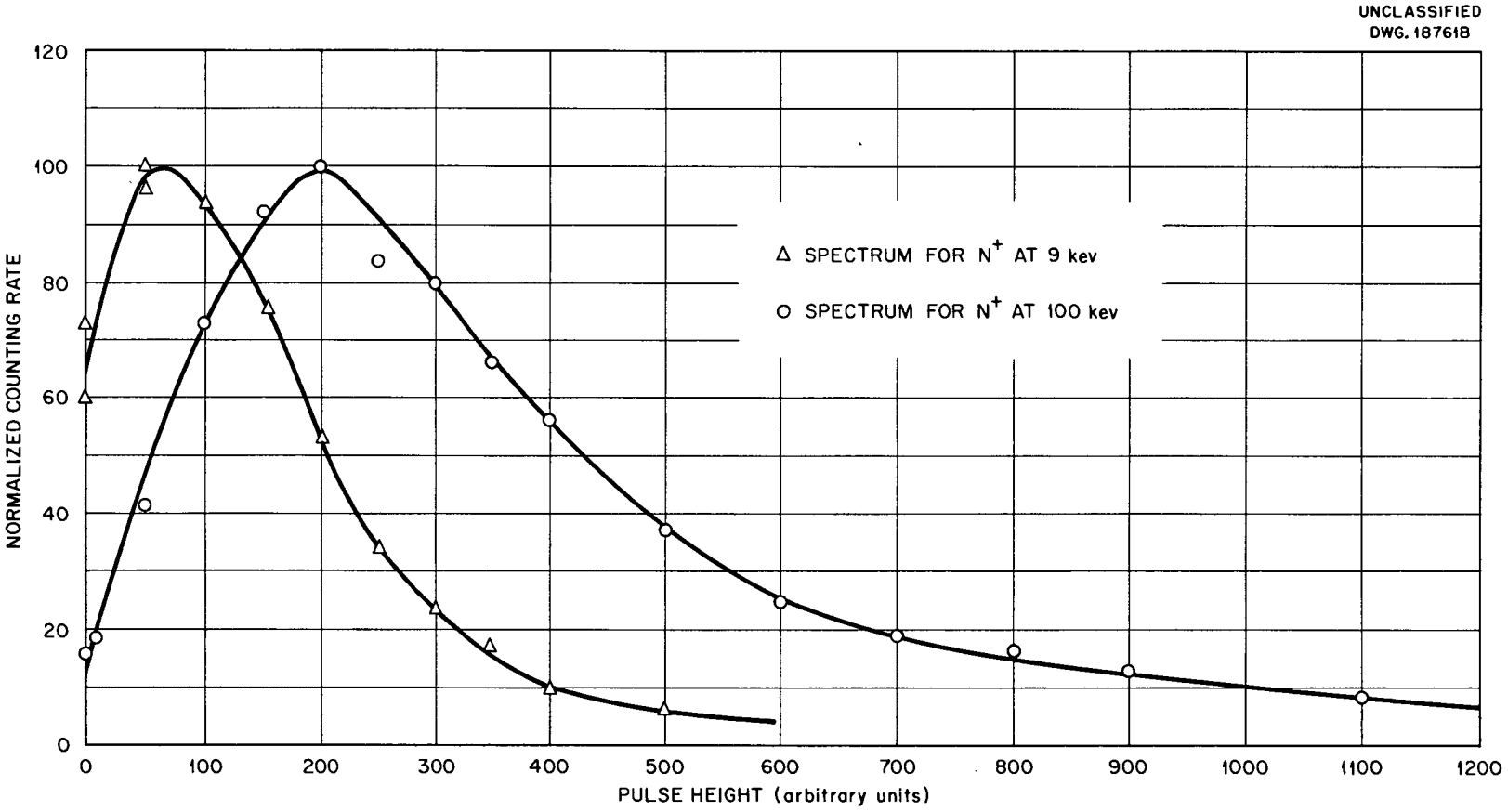

Fig. 26. Pulse Spectrum from Electron Multiplier.

To determine the maximum counting rate before losses became excessive the efficiency was obtained for different counting rates and is shown in Fig. 27. The maximum counting rate permissible before losses became very large is 80,000 counts/sec, which corresponds to an input ion current of approximately 10^{-15} amperes. This observed decrease in efficiency is due to blocking of the external electronic circuits and not of the multiplier tube, as is readily seen by reference to the data displayed in Fig. 18. The 5% spread in data points is a result of the inaccuracy in the measurements of the input ion current.

The variation of efficiency with energy is shown in Fig. 28 for N^+ ions. The efficiency is 100% for energies greater than 10 kev. Below this value it decreases, being 92% at 4 kev.

The efficiency as a function of mass is shown in Fig. 29. For an energy of 10 and 100 kev the efficiency of all masses studied was 100%. Fig. 30 shows a slight shift in the pulse height maximum toward large pulse size for the diatomic ion of nitrogen over that of the monoatomic ion.

An attempt was made to determine the efficiency of the multiplier in the detection of neutral particles. The neutral particles were obtained by passing the positive ion beam through a region of gas. By a process of charge exchange a large per cent of the emergent beam was neutral atoms with essentially the initial energy. If the pulse spectra were the same both in shape and most probable pulse height, the efficiency would be the same for both neutrals and positive ions for the same mass and energy. The pulse spectra of N^o and N^+ at an energy of 52 kev is

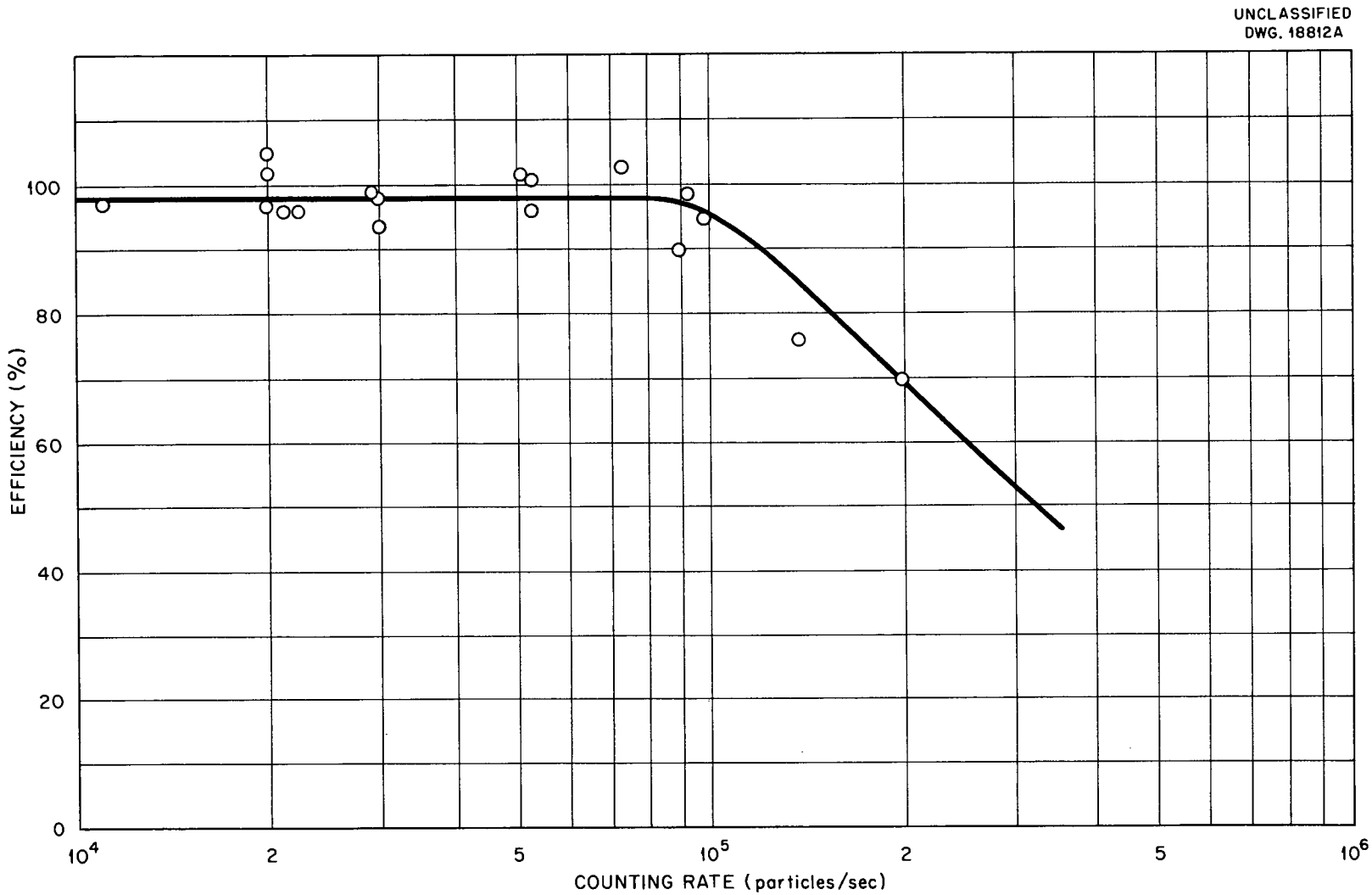

Fig. 27. Efficiency vs. Counting Rate; N^+; 100 kev.

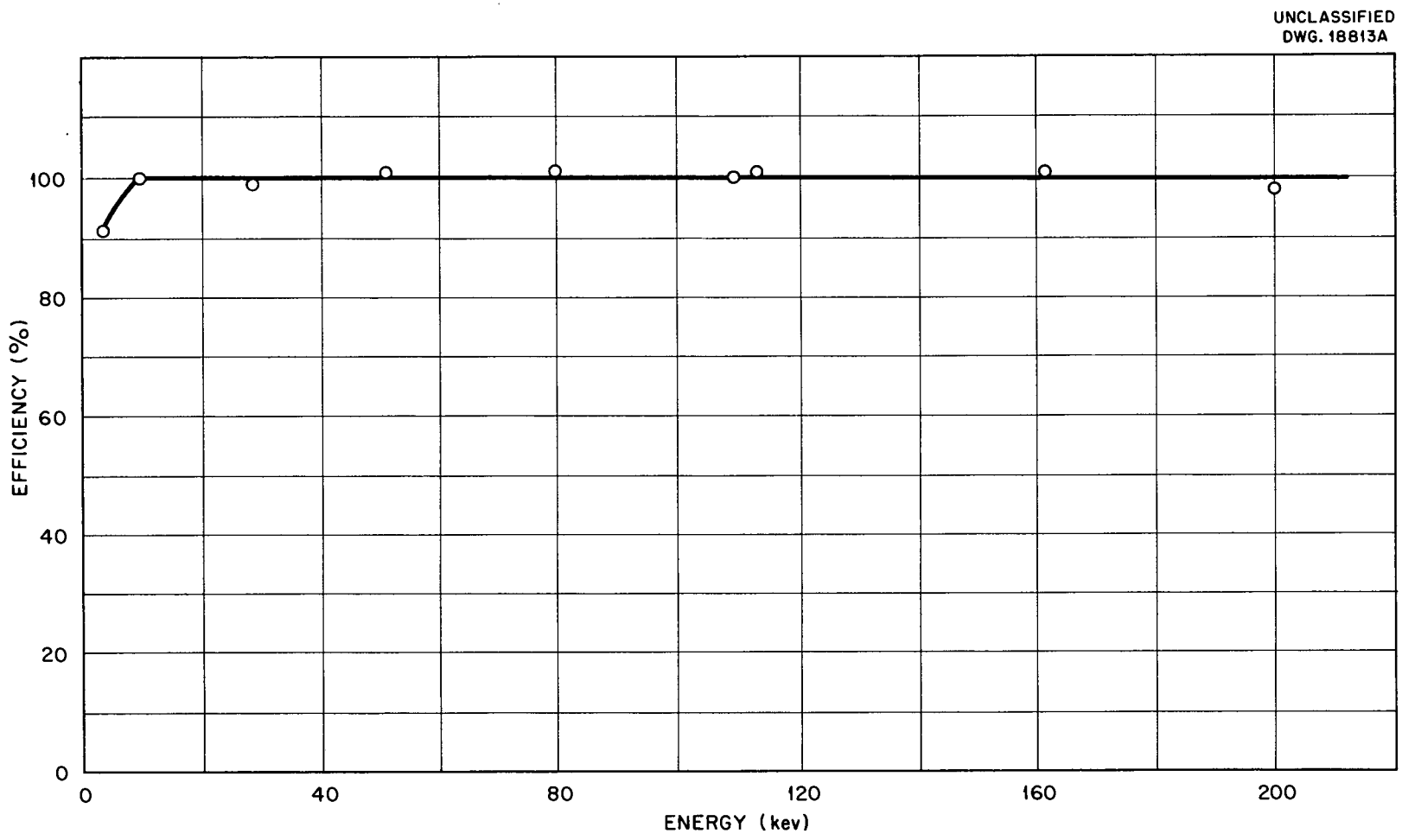

Fig. 28. Counting Efficiency vs. Energy, for N^+.

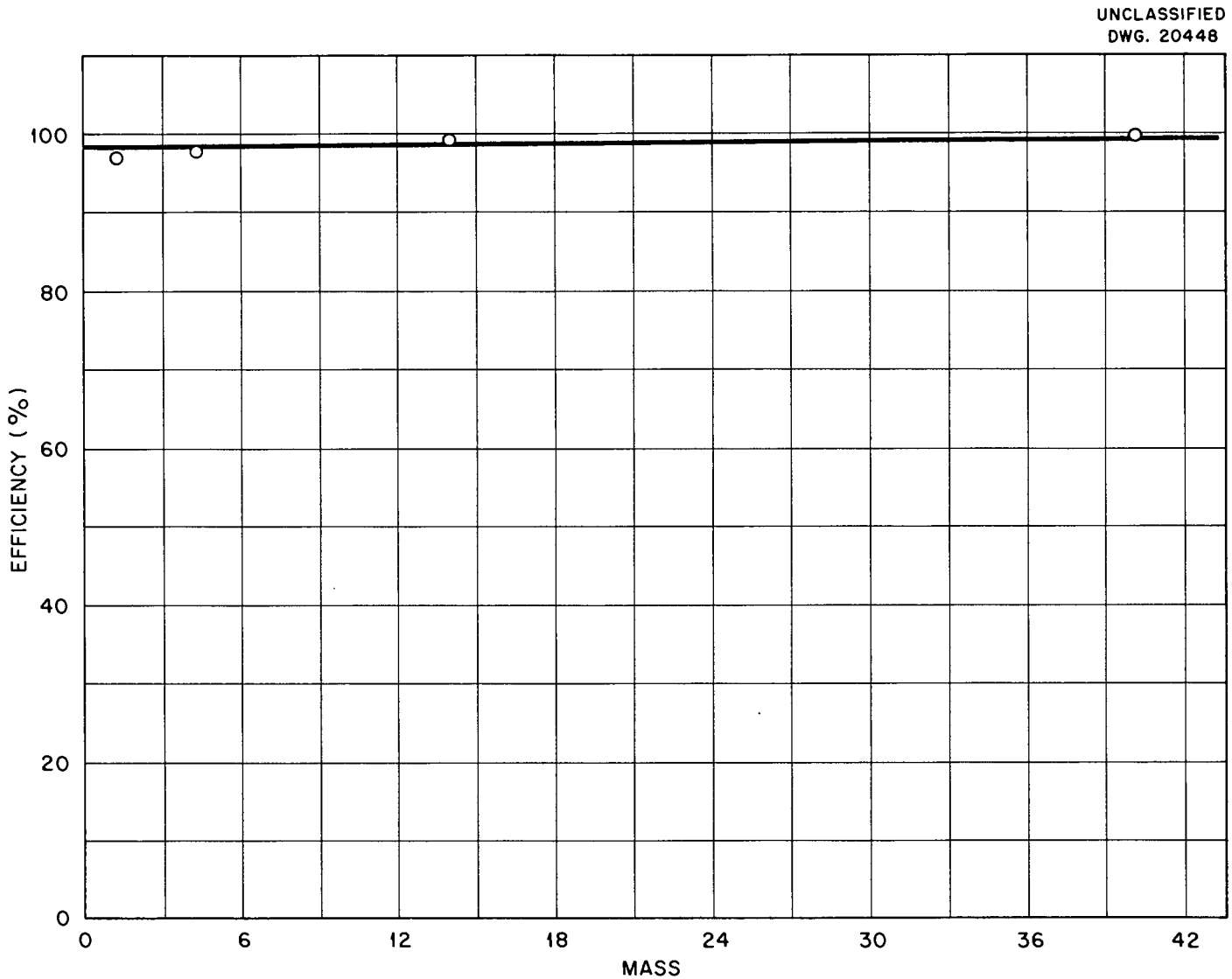

Fig. 29. Mass vs. Efficiency.

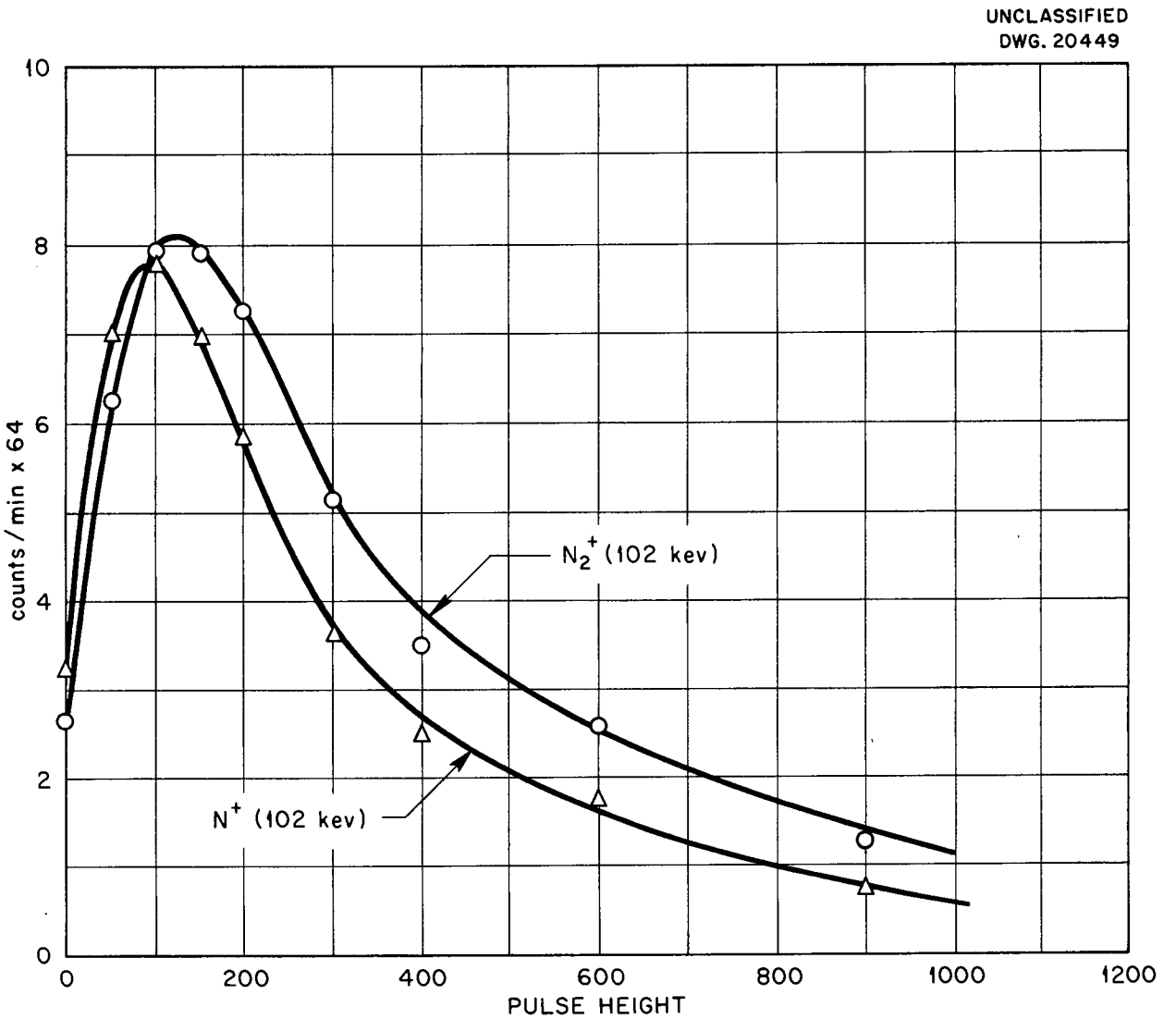

Fig. 30. Pulse Spectrum for N_2^+ and N^+.

shown in Fig. 31. The average pulse height is approximately 10% smaller for the neutral atoms. Additional work must be done to definitely establish that the multiplication of the multiplier is less for the neutral particles. The efficiency of the multiplier for counting the neutrals is 100% if the discriminator setting is sufficiently low to insure the pulse spectrum curve to be above the value selected for the bias setting (the same criterion as used for ion counting).

In all the measurements an absolute knowledge of the error of the measurements is unknown. The high voltage measurement is known to within five per cent. All the calibrations of the electrometers used are accurate to within 2%. The greatest source of error arises due to the fluctuations in the positive ion beam during the measurement. In all cases where it was obvious the beam varied the measurement was discarded. In this manner repeatable results could be obtained within a range of five per cent. The multiplier efficiency as stated is believed to be accurate within this five per cent.

Conclusions.

As a relative detector the electron multiplier is an excellent choice for measuring positive ions. It is also a reliable quantitative detector if proper care is taken. The efficiency for counting positive ions of an energy greater than 10 kev can be made 100 $\pm$ 0%. The gain of the multiplier for high energies increases as the mass increases with the exception of such ions as neon. Positive ion currents as large as 10^{-15} amperes may be detected with high speed counting circuits. Dynode aging has very little effect on the gain of the multiplier. The multiplier is

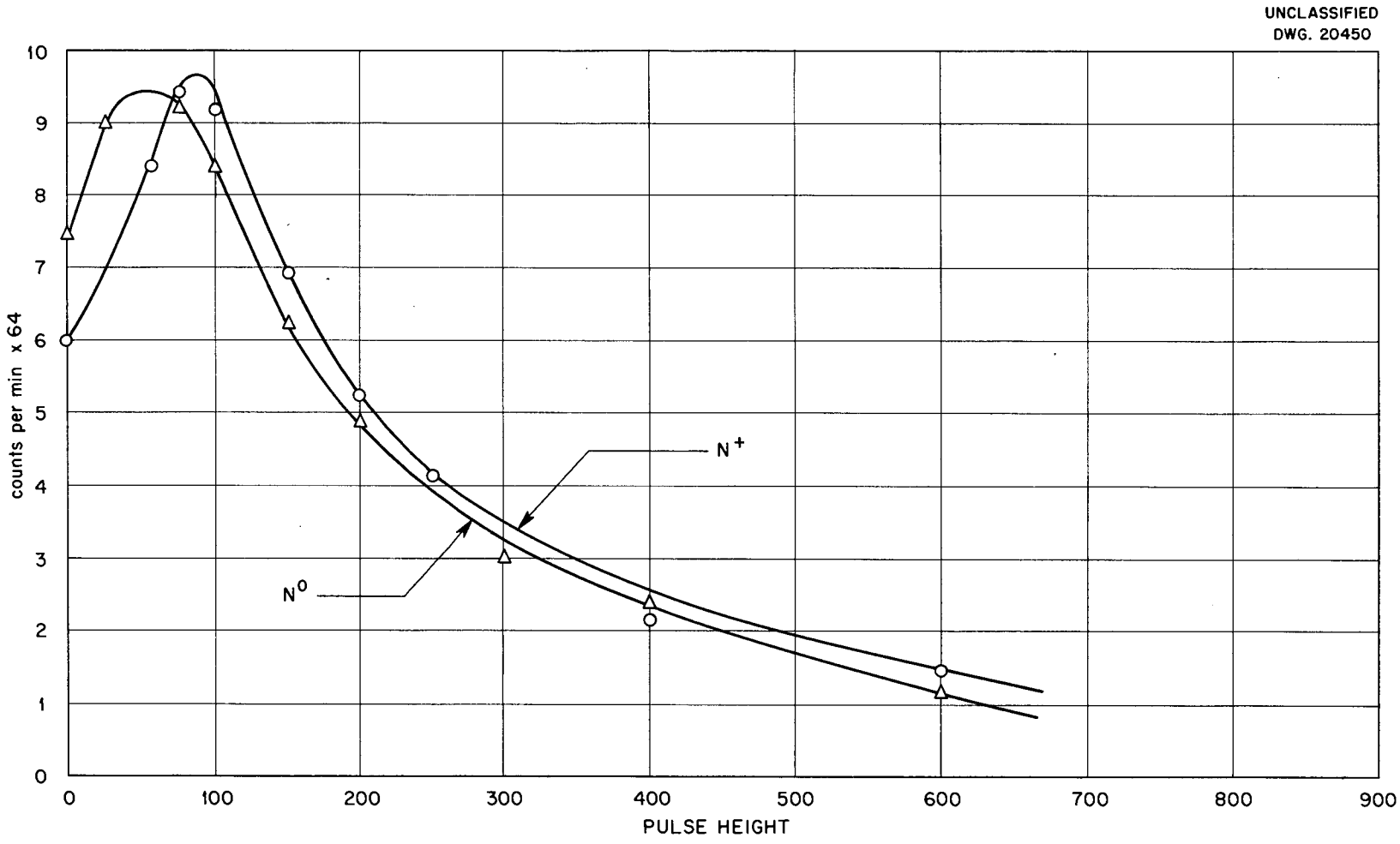

Fig. 31. Pulse Spectrum for Positive Ions and Neutrals of Nitrogen at 52 kev.

pressure independent below 10^{-4} mm Hg. The determination of efficiency should be made by an analysis of the pulse spectra before using the multiplier. The phenomena of secondary emission are dependent to some extent upon velocity. The secondary electron multiplier may be a very useful detector of neutral particles, however, more work must be done to determine the yields from atoms.

BIBLIOGRAPHY

BIBLIOGRAPHY

Ahern, A. J. "The Emission of Secondary Electrons from Tungsten," Physical Review 38, 1858-1870 (1931).

Allen, J. S. "The Detection of Single Positive Ions, Electrons and Photons," Physical Review 55, 966-971 (1939).

Allen, J. S. "An Improved Electron Multiplier Particle Counter," Review of Scientific Instruments 18, 739-749 (1947).

Allen, J. S. "Particle Detection with Multiplier Tubes," Nucleonics 3, 34-39 (1948).

Allen, J. S. "The X-Ray Photon Efficiency of a Multiplier Tube," Review of Scientific Instruments 12, 484-488 (1941).

Allen, J. S. "Recent Applications of Electron Multiplier Tubes," Preliminary Report No. 10, National Research Council.

Allen, J. S. "Experimental Evidence for the Existence of a Neutrino," Physical Review 61, 692-697 (1942).

Allen, J. S. "Characteristics of Metal Type Electron-Multiplier Tube," MDDC-275 (1944).

Barnett, C. F., Stier, P. M., and Evans, G. E. "The PIG Ion Source," Review of Scientific Instruments (May, 1953).

Baroody, E. M. "A Theory of Secondary Emission from Metals," Physical Review 78, 780-787 (1950).

Bay, Z. "Electron Multiplier as an Electron Counting Device," Nature 141, 284 (1938).

Bell, P. R., and Jordan, W. H. "Scintillation Counters," Nucleonics 5, 30-41 (1949).

Blaur, M., and Dreyfus, B. "The Multiplier Photo-Tube in Radioactive Measurements," Review of Scientific Instruments 16, 245-248 (1945).

Bruining, H. "Absorption of Secondary Electrons," Physica 5, 901-912 (1938).

Bruining, H. "Secondary Electron Emission Caused by Bombardment with Slow Primary Electrons," Physica 5, 913-917 (1938).

Bruining, H. "Secondary Electron Emission," Philips Technical Review 3, 80 (1938).

Bruining, H. "The Secondary Emission of Solids," Springer, Berlin.

Bruining, H., and DeBoer, J. H. "Secondary Electron Emission of Metals with a Low Work Function," Physica 4, 473-477 (1937).

Bruining, H., and DeBoer, J. H. "Secondary Electron Emission," Physica 6, 834-839 (1938).

Bruining, H., and DeBoer, J. H. "Secondary Electron Emission of Metals," Physica 5, 17-30 (1938).

Coltman, J. W., and Marshel, F. H. "Photo-Multiplier Radiation Detector," Nucleonics 1, 58-64 (1947).

D'Ano, A. M., Da Rios, R., and Malaspina, L. "Liberation of Electrons from Metallic Surfaces by the Impact of Ions," Nuovo Cimento 5, 394-398 (1948).

Dare, J. A., and Rower, W. H. "Construction and Test of an Electron Multiplier Alpha Particle Detector," Technical Report No. 6, Office of Naval Research.

Darrow, K. K. Electrical Phenomena in Gases, Baltimore: Williams and Williams Company, 1932.

Eisenstein, A., and Gingrich, N. S. "Electron Multiplier and Photographic Film for Detecting X-Rays -- A Comparison Between a G-M Counter and Electron Multipliers," Review of Scientific Instruments 12, 582-586 (1941).

Farago, P. S. "Electron Multiplier Tube of Large Effective Cathode," Nature 161, 60 (1948).

Farnsworth, H. E. "Electronic Bombardment of Metal Surfaces," Physical Review 25, 41-57 (1925).

Green, D. "Secondary Electron Emission from Mo Produced by Helium, Argon, and Hydrogen," Proceedings of Physical Society of London B63, 876-889 (1950).

Hagstrum, H. E. "Electron Ejection from Mo by He^{+}, He^{++}, and He_2^{++}," Physical Review 89, 244 (1953).

Harris, J. H. O. "Secondary Electron Radiation," Electronics 17, 100-108 (1944).

Heale, M., and Chaffee, E. L. "Secondary Electron Emission from a Hot Nickel Target Due to Bombardment of Hydrogen Ions," Physical Review 49, 925-930 (1936).

Heale, M., and Houterman, C. "The Relative Secondary Electron Emission Due to Helium, Neon, and Argon Ions Bombarding a Hot Nickel Target," Physical Review 58, 608-610 (1940).

Heale, M. "Comparison of the Secondary Electron Emission Due to H_2^+ and D_2^+ Ions," Physical Review 55, 984 (1939).

Hill, A. G., Buechner, W. W., Clark, J. S., and Fisk, J. B. "The Emission of Secondary Electrons Under High Energy Positive Ion Bombardment," Physical Review 55, 463-470 (1939).

Jackson, W. J. "Secondary Emission from Mo Due to Bombardment by High Speed Positive Ions of the Alkali Metals," Physical Review 30, 473-478 (1927).

Kadyshevich, A. E. "Theory of Secondary Emission from Metals," Journal of Physics, USSR, 2, 115 (1940).

Kallman, H. "Scintillation Phosphors," Scintillation Counter Symposium, Oak Ridge National Laboratory, June 1949.

Kollath, R. "On the Secondary Electron Emission of Beryllium," Ann. Der. Physik 33, 285-299 (1938).

Lindford, L. H. "The Emission of Electrons by Swiftly Moving Mercury Ions," Physical Review 47, 279-282 (1935).

Massey, H. S. W., and Burhop, E. H. S. Electronic and Ionic Impact Phenomena, Oxford: Oxford University Press, 1952.

McKay, K. G. Advances in Electronics, New York: Academis Press, 1948.

Montgomery, C. G. "Counters for Cosmic Rays," Technical Report No. 2, Office of Naval Research, 1949.

Morrish, A. H., and Allen, J. S. "Performance of the Allen Type Multiplier Tube," Physical Review 74, 1260 (1948).

Oliphant, M. L. E. "The Liberation of Electrons from Metal Surfaces by Positive Ions," Proceeding of Royal Society of London, A127, 373-406 (1930).

Papp, G., and Sasvari, K. "The Application of Electron Multiplier Tubes in the Measurement of X-ray Beam Intensities and Crystal Structure," Journal of Applied Physics 19, 1182-1183 (1948).

Papp, G. "Determination of the Pulse Period of Electron Multiplier Tubes," Review of Scientific Instruments 19, 568-569 (1948).

Ploch, W. "Mass Dependence of Electron Emission by Isotropic Ions," Zeitschrift für Physik 130, 174-195 (1951).

Pomerantz, M. A., and Marshall, J. F. "Fundamentals of Secondary Electron Emission," Proceedings of Institute Radio Engineers 39, 1367-1373 (1951).

Pierce, J. R. "Electron Multiplier Design," Bell Laboratory Record 16, 305-309 (1938).

Rajchman, J. A., and Snyder, R. L. "An Electrically-Focused Multiplier," Electronics 13, 20-23 (1940).

Richard, P. I., and Hays, E. E. "Scintillation Type Ion Detector," Review of Scientific Instruments 21, 99-100 (1950).

Robson, J. M. "The Electron Multiplier as a Counter for 10-Kev Protons," Review of Scientific Instruments 19, 865-871 (1948).

Robson, J. M. "The Electron Multiplier as a Counter for 10-Kev Protons," CRP-383, National Research Council of Canada, 1948.

Rosario, L. D. "Use of an Electron Multiplier Tube as a New Technique in Disintegration Experiments," Physical Review 74, 304-314 (1948).

Rudberg, E. "Inelastic Scattering of Electrons from Solids," Physical Review 50, 138-158 (1936).

Shockley, W., and Pierce, J. R. "A Theory of Noise for Electron Multipliers," Proceedings of Institute Radio Engineers 26, 321-332 (1938).

Smith, L. "Magnetic Electron Multipliers for Detection of Positive Ions," AECU-1057 (1950).

Snell, A. H., and Miller, L. C. "The Secondary Electron Multiplier as a Particle Counter, AECD-1956.

Stoddart, H. "Report on an Electron Multiplier," AECU-564.

Stone, R. P. "A Secondary Emission Electron Multiplier for the Detection of High Energy Particles," Review of Scientific Instruments 20, 935-941 (1949).

Suhrman, R., and Kundt, W. "The Secondary Emission of Pure Metallic Films in the Ordered and Unordered States and Their Transparency for Secondary Electrons," Z. Phys. 120, 363-382 (1943).

Trelor, L. R. G., and Landon, D. H. "Secondary Electron Emission from Nickel, Cobalt, and Iron as a Function of Temperature," Proceedings of the Physical Society of London 50, 625-633 (1938).

Trump, J. G., and Van de Graaff, R. J. "The Secondary Emission of Electrons by High Energy Electrons," Physical Review 75, 44-45 (1949).

Webster, E. W., Van de Graaff, R. J., and Trump, J. G. "Secondary Electron Emission from Metals by Positive Ion Bombardment in High Extraction Fields," Journal of Applied Physics 23, 264-266 (1952).

Woodward, W. Introduction to Nuclear Physics, Lectures at Massachusetts Institute of Technology, 1947.

Wooldridge, D. E. "Theory of Secondary Emission," Physical Review 56, 562-578 (1939).

Wooldridge, D. E. "Temperature Effects in Secondary Emission," Physical Review 58, 316-321 (1940).

Wooldridge, D. E., and Hartman, C. D. "The Effects of Order and Disorder on Secondary Electron Emission," Physical Review 58, 381 (1940).

Zworykin, V. K., Morton, G. A., and Malter, L. "The Secondary Emission Multiplier -- A New Electronic Device," Proceedings of Institute of Radio Engineers 24, 351-375 (1936).

Zworykin, V. K., and Rajchman, J. A. "The Electrostatic Electron Multiplier," Proceedings of the Institute of Radio Engineers 27, 558-566 (1939).

Zworykin, V. K., Ruedy, J. E., and Pike, E. W. "Silver Magnesium Alloy as a Secondary Electron Emitting Material," Journal of Applied Physics 12, 696-698 (1941).